U.PORTO

MESTRADO
QUÍMICA FARMACÊUTICA

Aminothioxanthonic Derivatives: Synthesis and Study of Antifungal Synergistic Effect

Filipa Daniela Freitas Barbosa

M
2019

U.PORTO **Filipa Daniela Barbosa.** Aminothioxanthonic Derivatives: Synthesis and Study of Antifungal Synergistic Effect **M.**FFUP **2019**

Aminothioxanthonic Derivatives: Synthesis and Study of Antifungal Synergistic Effect

Filipa Daniela Freitas Barbosa

FACULDADE DE FARMÁCIA

Filipa Daniela Freitas Barbosa

Aminothioxanthonic Derivatives: Synthesis and Study of Antifungal Synergistic Effect

Dissertation presented to the Faculdade de Farmácia da Universidade do Porto, to obtain the degree of Master in Pharmaceutical Chemistry.

Work developed under the scientific supervision of Professor Doctor Maria Emília Pereira de Sousa and Professor Doctor Maria Eugénia Ribeiro Pinto.

July, 2019

Advisor

Prof. Dr. Emília Sousa

Co-advisor

Prof. Dr. Eugénia Pinto

Master Course Director

Prof. Dr. Emília Sousa

This work was developed in the Centro de Química Medicinal da Universidade do Porto-CEQUIMED-UP, Laboratório de Química Orgânica e Farmacêutica, Departamento de Ciências Químicas, Faculdade de Farmácia da Universidade do Porto, and Laboratório de Microbiologia, Departamento de Ciências Biológicas, Faculdade de Farmácia da Universidade do Porto. Support for this work was provided by the Strategic Funding UID/Multi/04423/2019 and under the project PTDC/SAU-PUB/28736/2017 (reference POCI-01-0145-FEDER-028736) , co-financed by COMPETE 2020, Portugal 2020 and the European Union through the ERDF and by FCT through national funds, as well as CHIRALBIOACTIVE-PI-3RL-IINFACTS-2019 .

Poster Communications

Some results presented in this dissertation are part of the following scientific poster communications:

6. F. Durães*, **F. Barbosa**, J. Freitas-da-Silva, S. Cravo, P. Costa, M. Pinto, E. Sousa. From the computer to the lab bench: design, synthesis and synergistic activity with antibacterial drugs of aminated thioxanthones. EUROPIN Summer School on Drug Design – Vienna, Austria, September 15-20, 2019. (submitted)

5. F. Durães*, **F. Barbosa**, M. Pinto, E. Sousa. Unforeseen tandem Ullmann type C–N coupling and dehydrative cyclization of a thioxanthone and guanidine. XXVI Encontro Nacional da Sociedade Portuguesa de Química, Porto, Portugal, July 24 - 26, 2019.

4. **F. Barbosa***, F. Durães, E. Pinto, M. Pinto, E. Sousa. Synthesis of thioxanthone derivatives to revert drug resistances. 4ª Edição da Escola de Inverno de Farmácia, Porto, Portugal, March 18-27, 2019.

3. F. Durães*, **F. Barbosa**, M. Pinto, E. Sousa. Synthesis of aminated thioxanthones as agents to circumvent antimicrobial resistance. 4ª Edição da Escola de Inverno de Farmácia, Porto, Portugal, March 18-27, 2019.

2. **F. Barbosa***, F. Durães, E. Pinto, M. Pinto, E. Sousa. Synthesis of thioxanthones as potential inhibitors o efflux pumps. 12.º Encontro de Investigação Jovem da Universidade do Porto, Porto, Portugal, February 13-15, 2019, p. 308.

1. F. Durães, **F. Barbosa***, E. Pinto, M. Pinto, E. Sousa. Halogen-exchange and amination of chlorinated thioxanthones. XXIV Encontro Luso-Galego de Química, Porto, Portugal, November 21-23, 2018, p. 448.

* Presenting author

Acknowledgements

First of all, I would like to acknowledge all the Professors at the Laboratory of Organic and Pharmaceutical Chemistry of the Faculty of Pharmacy that helped me to acquire all necessary skills to my success.

I would like to express my enormous gratitude to my supervisor Professor Emília Sousa, for allowing me to take part in this research project, which has been a major learning experience, and for her support and guidance in the supervision of the work. In the most difficult moments, Professor Emilia Sousa was always present, encouraged me, supported me and provided me valuable teachings.

I wish to express my sincere thanks to my co-supervisor Professor Eugénia Pinto, for giving me the opportunity to test biologically the thioxanthonic derivatives and to acquire a better knowledge of this scientific area at experimental and theoretical level. I would like to acknowledge her guidance, continued support and her availability.

I would also like to thank Dr. Sara Cravo for the technical assistance in microwave synthesis and for performing HPLC analysis on the compounds.

I am also grateful to Liliana and Gisela for assisting me in many different ways. I also thank you for the kindness and friendliness that always treated me.

To MsC Fernando Durães my gratitude for supporting and helping during the laboratorial work. I would also like to thank his for friendship and for all patience that he showed during this year.

To MsC Joana Freitas-da-Silva for supporting and helping me in biological activity part and for contributing to the development of my knowledge in this area.

My sincere thanks to my lab colleagues and to my colleagues of Master's Degree of Pharmaceutical Chemistry, for their friendship, support and for sharing skills.

Finally, I would like to thank my family, with special attention to my parents and sister, for all their emotional support, understanding, love and affection which are very important to force me to get successes.

Abstract

The rise and spread of antifungal drug resistance present one of the most pressing health issues of our days. This fact, allied with the relatively few classes of antifungal drugs, makes it necessary to develop new therapeutic strategies. The resistance by fungi can arise due to a multiplicity of factors, including the increase of drug efflux pumps. The fungal efflux pumps, ATP-binding cassette (ABC) and major facilitator superfamily (MFS), promotes the outward transport of drugs, causing the development of resistance to antifungals in fungi.

One approach to overcome this resistance is through efflux pump inhibition. Thioxanthones, dibenzo-gamma-thiopyrones, are an important class of molecules showing interesting biological properties, including efflux pump inhibition. Based on these considerations, this scaffold was selected for further studies within the scope of finding new efflux pump inhibitors.

In this dissertation, five amino thioxanthonic derivatives (**Tx's 2**, **4**, **5**, **7**, and **11**) were synthesized by Ullmann cross coupling reaction between the thioxanthone derivatives 1-chloro-4-propoxy-9*H*-thioxanthen-9-one (**TxCl**) or the 1-bromo-4-propoxy-9*H*-thioxanthen-9-one (**TxBr**) and amine building blocks (**A 2**, **4**, **5**, **7** and **11**). The structure elucidation of the synthesized compounds was carried out by spectroscopic methods, including IR, NMR (^{1}H, ^{13}C, HMBC and HSQC), and their purity evaluated by HPLC.

The antifungal synergy effects of the obtained compounds (**Tx's 2**, **4**, **5**, and **7**) and three other structure related thioxanthonic derivatives (**TxOMe**, **TxA1**, and **Tx53**) previously synthesized in our research group, with two azoles, fluconazole (FLC) and voriconazole (VOR), were studied. The compounds were tested against three *Candida* stains with different susceptibility profiles to azoles, by the checkerboard method according Clinical and Laboratory Standards Institute (CLSI). In addition, we also evaluated potential synergism between the two azoles (FLC and VOR) and the antiarrhythmic drug amiodarone (AMD), since this drug has shown antifungal activity when administered in combination with azoles. The evaluation of drug interaction was determined by calculating the fractional inhibitory concentration (FIC).

Among the seven tested compounds, only the amino-thioxanthonic derivative **TxA1** showed promising antifungal activity against the three *Candida* strains. However, none of the synthesized compounds showed synergistic antifungal effect with azoles against the tested yeasts. These results suggest that the tested thioxanthonic derivatives were not able to reverse antifungal resistance.

Concerning amiodarone when combined with azoles, this drug not only exhibited synergistic growth inhibition of azole-resistant *Candida albicans* H37, with a fractional inhibitory concentration index (FICI) of 0.40, but also showed a reduction of the minimum

inhibitory concentration (MIC) values on the *C. albicans* strain that showed the trailing growth effect. These results suggest the possibility of combining AMD with azoles to treat invasive fungal infections.

Keywords: thioxanthones, antifungal drug resistance, efflux pumps, ABC and MFS transporters, azoles, antifungal activity.

Resumo

A resistência a antifúngicos é um dos problemas de saúde mais urgentes nos dias de hoje. Este facto, associado ao reduzido número de classes de antifúngicos, torna necessário o desenvolvimento de novas estratégias terapêuticas. A resistência a antifúngicos pode surgir devido a uma multiplicidade de fatores, incluindo o aumento da expressão de bombas de efluxo. As bombas de efluxo fúngicas, ATP-*binding cassette* (ABC) e *major facilitator superfamily* (MFS), promovem o transporte de fármacos para o exterior das células, levando ao desenvolvimento de resistência a antifúngicos nos fungos.

Uma abordagem para superar esta resistência é através da inibição das bombas de efluxo. As tioxantonas, dibenzo-gama-tiopironas, são uma importante classe de moléculas que exibem propriedades biológicas interessantes, incluindo a inibição de bombas de efluxo. Tendo isso em consideração, esta estrutura foi selecionada para estudos no âmbito da descoberta de novos inibidores de bombas de efluxo.

Neste trabalho, cinco derivados tioxantónicos aminados (**Tx's 2**, **4**, **5**, **7**, e **11**) foram sintetizados por reação de acoplamento de Ullmann entre a 1-cloro-4-propoxi-9*H*-tioxanten-9-ona (**TxCl**) ou a 1-bromo-4-propoxi-9*H*-tioxanten-9-ona (**TxBr**) e os blocos construtores aminados (**A 2**, **4**, **5**, **7** e **11**). A elucidação estrutural dos compostos sintetizados foi realizada por métodos espectroscópicos, incluindo IV, RMN (^{1}H, ^{13}C, HMBC e HSQC), e a sua pureza foi avaliada por HPLC.

Os efeitos sinérgicos dos compostos obtidos (**Tx's 2**, **4**, **5** e **7**) e de três outros derivados tioxantónicos (**TxOMe**, **TxA1** e **Tx53**) sintetizados anteriormente no nosso grupo de investigação, com dois azóis, fluconazol (FLC) e voriconazol (VOR) foram estudados. Os compostos foram testados contra três estirpes de *Candida* com diferentes perfis de suscetibilidade aos azóis segundo o método *checkerboard* de acordo com as normas do Instituto de Normas Clínicas e Laboratoriais (CLSI). Além disso, também avaliamos o potencial sinergismo entre os dois azóis (FLC e VOR) e o antiarrítmico amiodarona (AMD), uma vez que este fármaco têm mostrado atividade antifúngica em combinação com azóis. A avaliação da interação entre os fármacos foi determinada pelo cálculo da concentração inibitória fracional (FIC).

Entre os sete compostos testados, apenas o derivado amino-tioxantónico **TxA1** apresentou atividade antifúngica promissora contra as três estirpes de *Candida* spp. No entanto, nenhum composto sintetizado apresentou sinergismo com azóis contra as três leveduras testadas. Esses resultados sugerem que os derivados tioxantónicos testados não foram capazes de reverter a resistência a antifúngicos.

Relativamente à amiodarona, quando combinada com os azóis, não apenas exibiu efeito sinérgico contra a *Candida albicans* H37 resistente a azóis, mas também mostrou

uma redução dos valores da concentração inibitória mínima (CIM) na estirpe *C. albicans* que exibe o efeito *trailing growth*. Estes resultados sugerem a possibilidade de combinar a AMD com azóis para tratar infeções fúngicas invasivas.

Palavras-chave: tioxantonas, resistência a antifúngicos, bombas de efluxo, transportadores ABC e MFS, azóis, atividade antifúngica.

Index

Index of figures

Index of tables

Index of schemes

Abbreviations

^{13}C NMR – Carbon nuclear magnetic resonance

^{1}H NMR – Proton nuclear magnetic resonance

5-FC – 5-Fluorocytosine

A – Amine

ABC – ATP-binding cassette superfamily

ADP – Adenosine 5'-diphosphate

AmB – Amphotericin B

AMD – Amiodarone

ATCC – American Type Culture Collection

ATP – Adenosine 5'-triphosphate

brs – Broad singlet

CFU – Colony forming units

CLSI – Clinical and Laboratory Standards Institute

d – Doublet

dd – Double doublet

ddd – Double double doublet

DNA – Deoxyribonucleic acid

EPI – Efflux pump inhibitor

EUCAST – European Committee on Antibiotic Susceptibility Testing

FIC – Fractional inhibitory concentration

FICI – Fractional inhibitory concentration index

FLC – Fluconazole

HMBC – Heteronuclear multiple bond correlation

HPLC – High performance liquid chromatography

HSQC – Heteronuclear single quantum coherence

IR – Infrared

J – Coupling constant

m – Multiplet

m.p. – Melting point

MDR – Multidrug resistance

MFS – Major facilitator superfamily

MIC – Minimum inhibitory concentration

MRP – Multidrug resistance-associated protein subfamily

NBD – Nucleotide binding domain

NMR – Nuclear magnetic resonance

p – Quintet

PDR – Pleiotropic drug resistance superfamily

P-gp – P-glycoprotein

$PhNO_2$ – Nitrobenzene

q – Quartet

RNA – Ribonucleic acid

s – Singlet

SPE – Solid phase extraction

st – Sextuplet

t – Triplet

TLC – Thin-layer chromatography

TMD – Transmembrane domains

TMS – Transmembrane segment

Tx – Thioxanthones

Tx 11 – 3-(9-Oxo-4-propoxy-9*H*-thioxanthen-1-yl)guanidine

Tx 2 – 6-Propoxythiochromeno[4,3,2-*de*]quinazolin-2(3*H*)-imine

Tx 4 – 1-((2,6-Difluorobenzyl)amino)-4-propoxy-9*H*-thioxanthen-9-one

Tx 5 – 2-((6-Propoxythiochromeno[4,3,2-*de*]quinazolin-3-ium-2(3*H*)-ylidene)amino)acetate

Tx 7 – *N*-(3-(3,4-Dichlorophenoxy)propyl)-6-propoxythiochromeno[4,3,2-*de*]quinazolin-2(3*H*)-imine

Tx53 – 1-(4-Acetylpiperazin-1-yl)-4-propoxy-9*H*-thioxanthen-9-one

TxA1 – 1-((2-(Diethylamino)ethyl)amino)-4-propoxy-9*H*-thioxanthen-9-one

TxBr – 1-Bromo-4-propoxy-9*H*-thioxanthen-9-one

TxCl – 1-Chloro-4-propoxy-9H-thioxanthen-9-one

TxOMe – 1-Methoxy-4-propoxy-9H-thioxanthen-9-one

UV – Ultraviolet

VOR – Voriconazole

Outline of the dissertation

The present thesis is structured in six chapters.

CHAPTER 1 – INTRODUCTION

In the first chapter, a brief introduction to thioxanthone derivatives will be given and their therapeutically activities will be highlighted in section 1.

A brief introduction about fungal infections, as well as the therapy that is currently used are presented in section 2. In section 2.2, is present a brief introduction of some key concepts about antifungal drug resistance. The ATP-binding cassette transporters (ABC) and major facilitator superfamily (MFS) commonly described as being involved in antifungal resistance are described on section 2.3, followed by a briefing on the use of efflux pump inhibitors to overcome drug resistance on section 2.4.

Finally, a description of the methods that are available for antifungal evaluation is presented on section 3.

CHAPTER 2 – AIMS

In the second chapter, the main objectives of the present work are described.

CHAPTER 3 - RESULTS AND DISCUSSION

This chapter focuses on the results and discussion of the developed research work, being subdivided in two sections. In the first part, the synthesis and the structure elucidation of the synthesized amino thioxanthonic derivatives will be presented. In the second part, the results concerning the antifungal evaluation of these derivatives are discussed.

CHAPTER 4 – CONCLUSIONS

The fourth chapter includes the main conclusions of the developed work.

CHAPTER 5 - MATERIAL AND METHODS

Chapter five describes the experimental methodologies used in this work and is divided in two parts; the first related with the synthesis and structure characterization of the new synthesized thioxanthones, and the second concerning the methods used to study the synergistic activity against *Candida* strains.

CHAPTER 6 – REFERENCES

In this chapter, the references cited throughout the thesis are presented. The references followed the American Chemical Society style guide. The main bibliographic research motors were ISI Web of Knowledge, from Thomson Reuters, Scopus, PubMed and Google Scholar.

CHAPTER I:
Introduction

I. Introduction

1. Thioxanthones

Thioxanthones belong to an important class of synthetic compounds, which have been showing interesting biological properties[1]. They are isosteric analogues of xanthones, consisting of *S*-heterotricyclic compounds which contain a dibenzo-gamma-thiopyrone scaffold[1]. The IUPAC numbering of the thioxanthone nucleus or 9*H*-thioxanthen-9-one is represented in **Figure 1**.

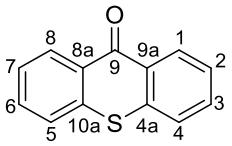

Figure 1 - Thioxanthone scaffold.

The first synthesis of a thioxanthone derivative was reported in 1891 when Graebe and Schultess were studying procedures for the synthesis of thioxanthenes[2]. The biological interest in this class of compounds started when lucanthone (Miracil D) (**Figure 2**), that appeared in the decade of the 1940, and its metabolite hycanthone (**Figure 2**) were introduced in clinic as antischistosomal agents[3-4]; but they were withdrawn from clinical use due to mutagenic side effects[4]. However, the interest in the mechanisms of action of these thioxanthones and their derivatives continued. Afterwards, lucanthone and hycanthone were also evaluated as antitumor agents[5] and, despite exhibiting significant antitumor properties[6], their mutagenicity[4] proscribed their use in cancer chemotherapy[7]. After chemical modification, SR271425 (**Figure 2**), a third-generation thioxanthone compound derived from hycanthone, was developed and entered phase I clinical trials based on robust *in vivo* antitumor activity, but it did not proceed due to its cardiotoxicity[8-10]. Nevertheless, these derivatives unleashed a big interest in the study of this class of compounds.

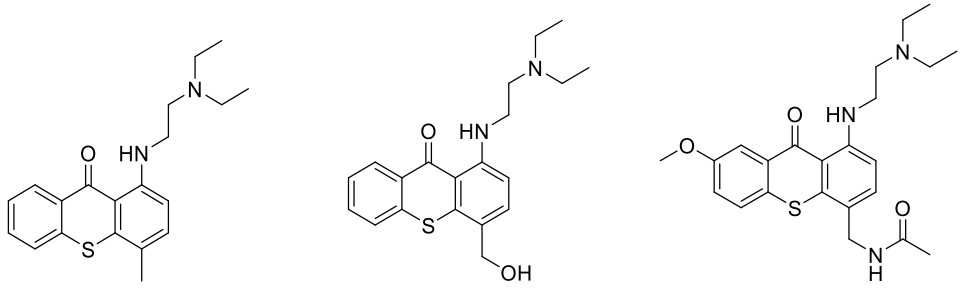

Lucanthone Hycanthone SR271545

Figure 2 - Structure of lucanthone, hycanthone, and SR271545.

Over the years, thioxanthone derivatives have been extensively synthesized and studied and photochemical properties and other biological activities were discovered, such as antischistosomal effects[11], antibacterial activity[12-13], monoamine oxidase inhibitory activity[14-15], antitumor activity[16-18], and efflux pump inhibition[18]. Due to the potential demonstrated by this scaffold to display several biological properties, as well as their proneness to chemical modifications, thioxanthones can be considered privileged structures[1], reason why several thioxanthonic derivatives have been synthesized and studied.

2. Fungal infections

The occurrence of fungal infections has risen dramatically over the past few decades, and they currently represent a global health threat. This increasing incidence of infection is influenced by the growing number of populations at risk, such as transplant recipients, cancer patients, and other individuals receiving immunosuppressive treatment[19].

Some fungal genera are naturally able to establish an infection in the healthy population and they are designated as primary pathogens. Other type of microorganisms responsible for fungal infections are the opportunistic pathogens. Opportunistic fungal pathogens, among them commensal fungi, are able to cause infections in immunocompromised individuals[20]. Fungal pathogens can be divided into three main groups, namely filamentous fungi, dimorphic fungi, and yeasts. Most of the primary pathogens are filamentous and dimorphic fungi, while most of the opportunistic pathogens are yeasts and filamentous fungi.

The severity of fungal infections differs from superficial infections to life-threatening systemic infections, when fungi get into the bloodstream of immunocompromised patients. The opportunistic human fungal pathogens most often associated with invasive fungal infections include *Candida*, *Aspergillus*, and *Cryptococcus*[21-22]. *Candida* species are the most common opportunistic fungal pathogens, being responsible for approximately 90% of

invasive infections. Among *Candida* spp., the opportunistic *Candida albicans* is the most frequent[22].

Furthermore, the opportunistic human fungal pathogens *C. albicans* and non-*albicans* species, such as *Candida glabrata*, *Candida parapsilosis*, *Candida tropicalis*, and *Candida krusei*, have acquired considerable significance in the recent past due to the enhanced susceptibility of fungal infections in immunocompromised patients[23]. Recently, the incidence of resistance to antifungals like azoles in both *C. albicans* as well as non-*albicans* species has increased considerably[23].

2.1. Antifungal agents

Despite extensive research dedicated to the development of new therapeutic strategies, there are only a few classes of antifungal agents used in medicine. There are four main antifungal drug classes used in clinical practice to treat essentially systemic fungal infections: azole derivatives, that inhibit the lanosterol 14α-demethylase, a key enzyme in ergosterol biosynthesis; echinocandins, that inhibit 1,3-β-glucan synthase; polyenes, that lead to an alteration of membrane function; and the drug 5-fluorocytosine, that causes aberrant ribonucleic acid (RNA) synthesis and interferes with deoxyribonucleic acid (DNA) replication[20, 24]. Several other classes, such as allylamines and thiocarbamates, that inhibit squalene epoxidase, an important enzyme in the biosynthesis of ergosterol from squalene[20, 24], are also used.

2.1.1. Azoles

Azole antifungals, discovered in late the 1960s, are by far the most commonly used systemic antifungal agents in clinical practice[25]. Azoles are synthetic cyclic organic molecules, that contain two main structures – a nitrogen-containing five membered ring and a halogenated benzene ring, both separated by one or more additional carbons and additional side chains. They can be classified as imidazoles (e.g., clotrimazole, econazole, miconazole, and ketoconazole) or triazoles (e.g., itraconazole and fluconazole) based on whether they have two or three nitrogens in the five-membered azole ring, respectively (**Figure 3**)[25-26].

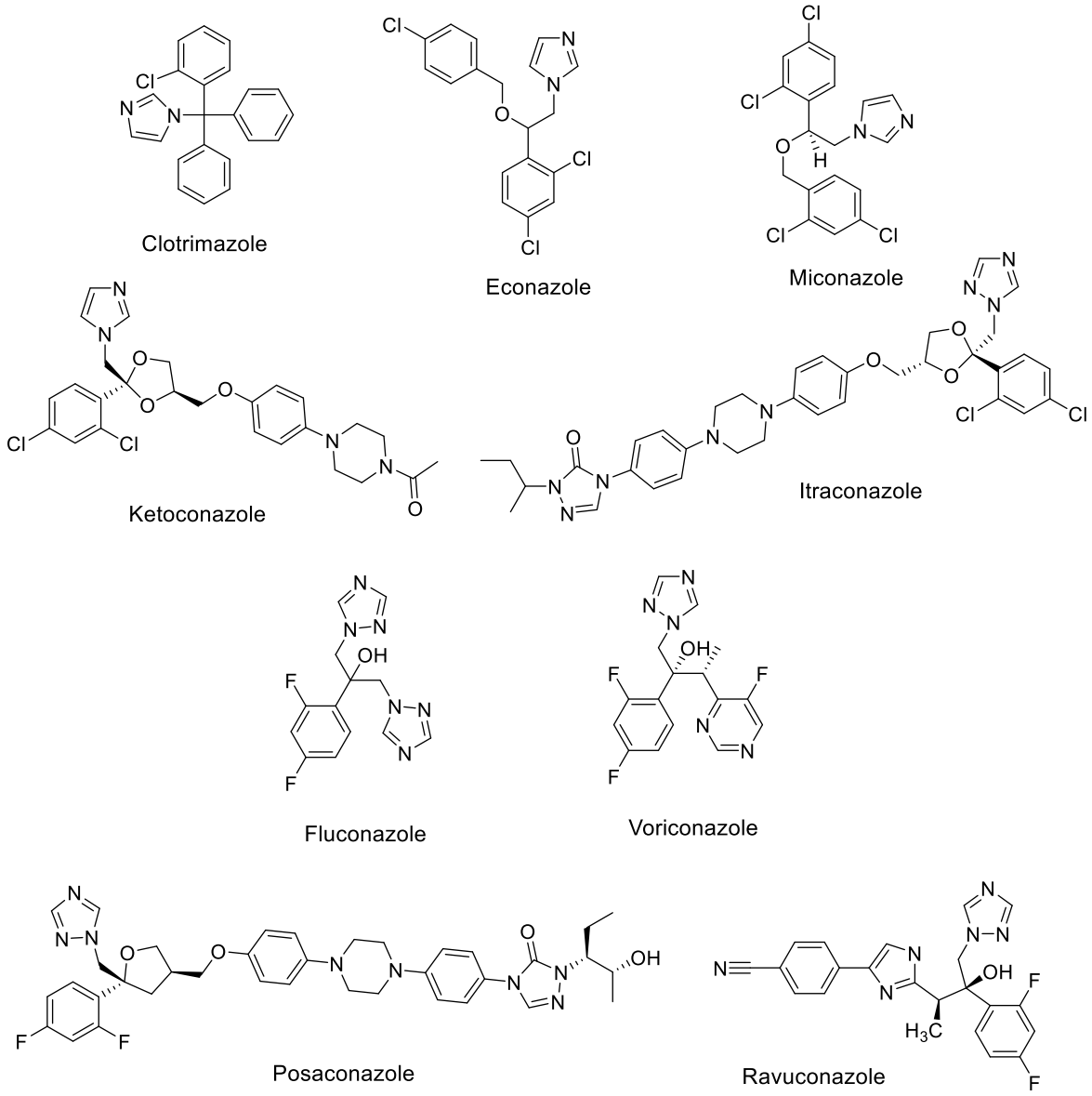

Figure 3 - Structures of the most commonly used azole antifungals, four imidazoles – clotrimazole, econazole, miconazole, and ketoconazole, two triazoles – itraconazole and fluconazole, and three triazoles – voriconazole, posaconazole, and ravuconazole.

The azole-based antifungal drugs target the ergosterol biosynthetic pathway by inhibition of a key enzyme, the lanosterol 14α-demethylase (encoded in *C. albicans* by the gene *ERG11*), inhibiting the conversion of lanosterol to ergosterol. Azole antifungal agents form, through their azole ring, a stoichiometric complex with the iron atom of the heme group of the enzyme. The resulting reduction ergosterol and the accumulation of lanosterol and other 14-methylated sterols interfere with the normal fungal membrane function, including alteration of cell membrane fluidity, reduction of the activity of membrane-associated enzymes and increases of fungal membrane permeability. In addition, accumulation of ergosterol precursors in the cell causes growth arrest[27-29].

Azoles possess a broad spectrum of activity against yeasts, such as *Candida* species, and molds. The first azole drugs developed were the imidazoles, which are generally used in topical formulations for superficial fungal infections, because of their toxicity or low bioavailability. First- and second-generation triazoles have a broader antifungal spectrum and better safety profile than imidazoles. The fluconazole (FLC), a first-generation triazole, has increased water solubility and improved pharmacokinetic properties but is ineffective against *Aspergillus fumigatus* and *C. krusei*. Itraconazole and voriconazole (VOR) are more effective and also fungicidal against *Aspergillus*, and the newer triazoles generation, such as posaconazole, ravuconazole, and albaconazole, appear to be effective against *Aspergillus* species, *Cryptococcus* species, Zygomycetes, and other fungi, such as *Malassezia* species[20].

2.1.2. Echinocandins

The fungal cell wall consists on polysaccharides as β-glucans, chitin, and mannoproteins. Some of the enzymes responsible for its synthesis are excellent targets for antifungal agents since they are not present in mammalian cells[27]. The disruption of the fungi cell wall polymers synthesis can lead to an osmotically instability, resulting in osmotic lysis[29].

Echinocandins are a class of antifungal drugs that demonstrate a unique and fungal-specific mode of action, while other antifungal drugs exert their effects primarily in the fungal cell membrane, the echinocandins inhibit cell wall synthesis[30]. They are semisynthetic amphiphilic lipopeptides composed for a cyclic hexapeptide core linked to a variably configured *N*-acyl-lipid side chain[31]. These antifungal compounds act by noncompetitive inhibition of the fungal enzyme 1,3-β-glucan synthase, thereby blocking the synthesis of 1,3-β-D-glucan, a key and critical cell wall component of many pathogenic fungi[32]. Together with chitin, the β-glucan are responsible for the cell wall's strength and shape. They are important in maintaining the structure and osmotic integrity of the cell wall[27].

Three drugs in this class, caspofungin, anidulafungin and micafungin (**Figure 4**), are currently available for clinical use[33]. Echinocandins are fungicidal against most *Candida* spp., namely *C. albicans*, *C. dubliniensis*, *C. glabrata*, and *C. krusei*; however, against *C. guilliermondii* and *C. parapsilosis* have higher minimum inhibitory concentrations (MIC)[33]. While they are highly effective against multiple *Candida* spp., including azole-resistant species and biofilms, the antifungal spectrum of echinocandins are essentially limited to *Candida* and *Aspergillus* spp. Consequently, they are limited in their clinical utility[27].

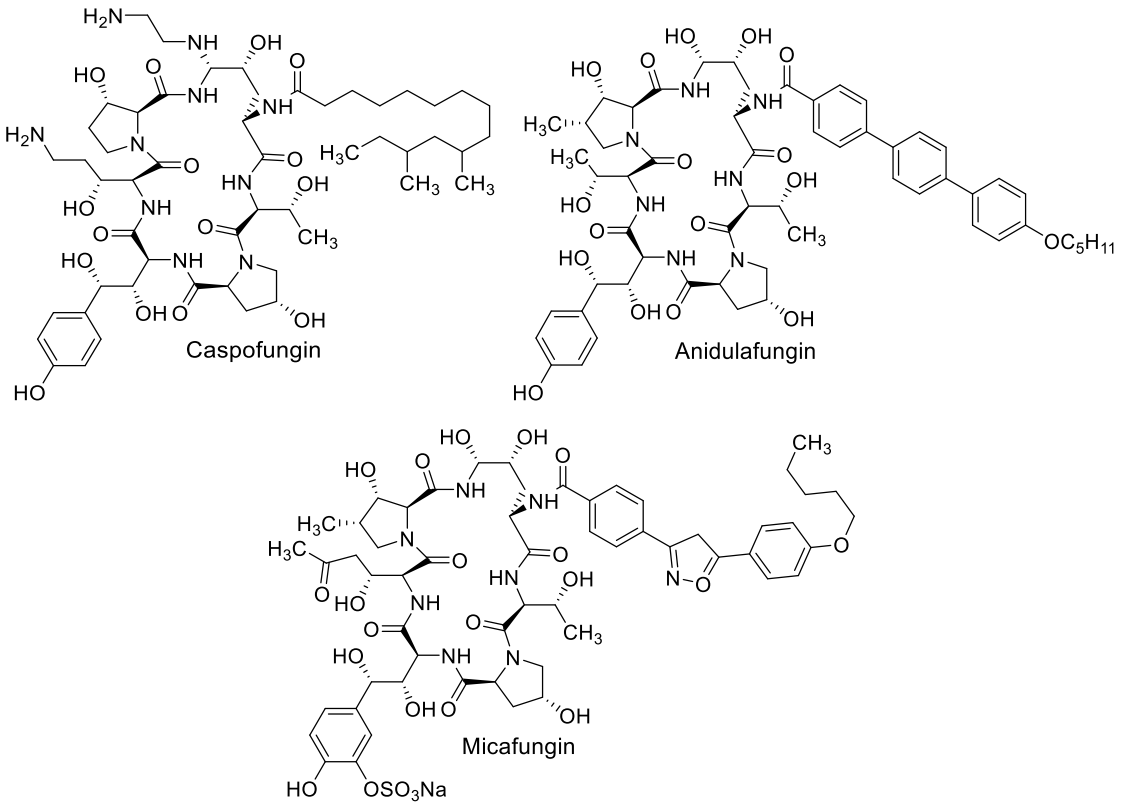

Figure 4 - Structures of echinocandins currently used in clinical practice.

2.1.3. Polyenes

The polyene antibiotics were the first introduced antifungal drugs for clinical use[29]. They are heterocyclic amphipathic organic molecules known as macrolides, produced by the *Streptomyces* species, that exhibit fungicidal activity. Polyenes have the broadest spectrum of activity of any clinically useful antifungal compounds[27, 34]. Agents belonging to the class of polyenes exert their antifungal activity by binding to ergosterol, the main sterol component of fungal membranes. These molecules bind the lipid bilayer and form pores that cause membrane disruption, increased permeability, leakage of ions from the cell, which ultimately results in cell death[27].

A large number of molecules belonging to the chemical class of polyenes have an antifungal activity; however, only three possess a toxicity allowing their use in clinical practice, namely amphotericin B (AmB), nystatin, and natamycine (**Figure 5**)[35].

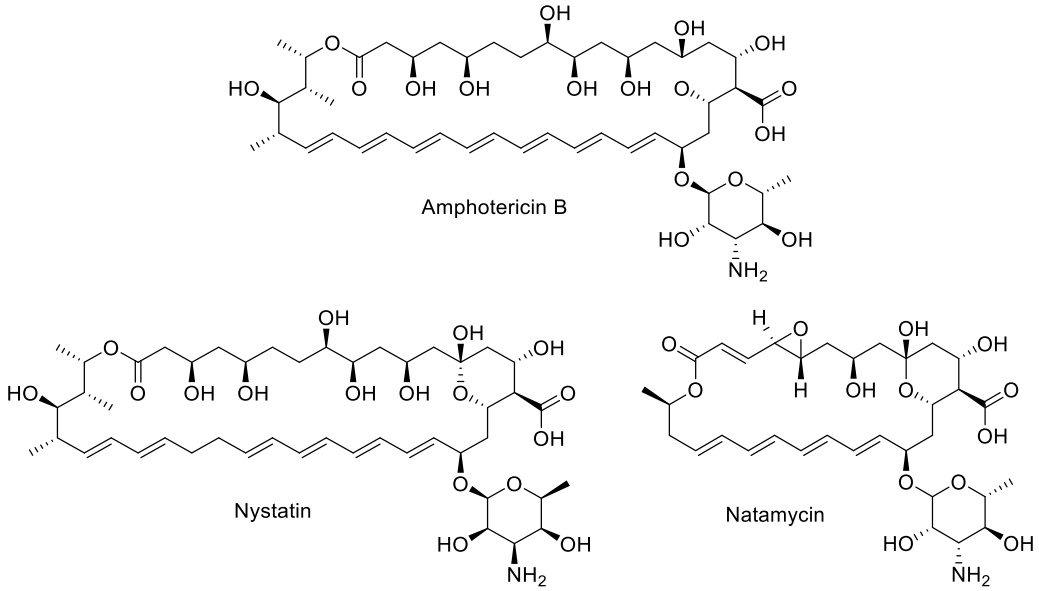

Figure 5 - Structures of the three main polyene drugs.

Nystatin is currently only used as a topical agent due to its high toxicity and low absorption. In contrast, AmB remains as the gold standard therapy, being a broad-spectrum antifungal polyene agent, that is active against most yeast and molds such as *Candida* spp., *Aspergillus* spp., *Cryptococcus neoformans*, Zygomycetes, dimorphic fungi, and some dematiaceous fungi[24, 34]. AmB binds to ergosterol and forms pores which leads to leakage of potassium ions and ergosterol sequestration, resulting in a disruption of the proton gradient[24, 36]. It also causes oxidative damage through the generation and accumulation of reactive oxygen species[24, 34]. Nephrotoxicity is the most important side effect for of the drug. This was due to interaction between AmB and cholesterol in the renal distal tubule membranes, causing tubular damage[34]. The side effects of AmB may be reduced in lipid formulations[27].

2.1.4. Fluorocytosine

The drug flucytosine or 5-fluorocytosine (5-FC), a fluorinated pyrimidine, has been used to treat fungal infections since the 1960's. It is a synthetic structural analog of the DNA nucleotide cytosine[35]. 5-FC was originally developed in the 1950's as an antitumor therapy but was found to be ineffective. Subsequent testing led to the discovered of its antifungal potential[35, 37].

5-FC is transported into the fungal cell by the enzyme cytosine permease, then cytosine deaminase converts 5-FC into 5-fluorouracil (5-FU) (**Figure 6**). Subsequent phosphorylation and incorporation of 5-FU into fungal RNA, cause miscoding and disruption of protein synthesis. Phosphorylated 5-fluorouracil also is co nverted to its deoxynucleoside,

fluorodeoxyuridine monophosphate, which blocks DNA synthesis by inhibiting the enzyme thymidylate synthase leading to the disruption of DNA replication[27].

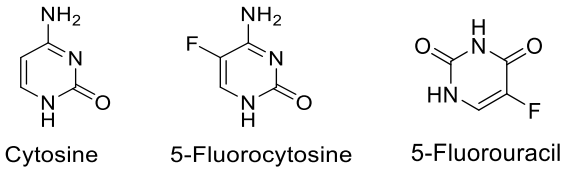

Figure 6 - Structures of cytosine, 5-fluorocytosine and 5-fluorouracil.

Flucytosine is active only against yeasts such as *Candida*, *Aspergillus*, and *Cryptococcus* species. For systemic infections including refractory invasive candidiasis and cryptococcal meningitis, it is administered in combination with other antifungal drugs, namely AmB, due to development of resistance to flucytosine during therapy of these infections[28].

2.1.5. Other antifungal agents

Besides the azoles, there are three additional minor ergosterol biosynthesis inhibitors which are used in therapy: allylamines, thiocarbamates, and morpholines. The allylamines and thiocarbamates, are reversible, noncompetitive inhibitors of squalene epoxidase, an enzyme responsible for the cyclization of squalene to lanosterol. Allylamines such as naftifine and terbinafine along with tolnaftate (**Figure 7**), a thiocarbamate, have found utility as antifungal agents in the clinic to treat dermatophyte infections. All drugs are used topically; terbinafine is also given orally for systemic absorption. The morpholines, apart from amorolfine (**Figure 7**), are only used in agriculture as fungicides. The mechanism of action of amorolfine, is described as inhibition of two different enzymes, the C14 sterol reductase and the C8 sterol isomerase inhibitors[35].

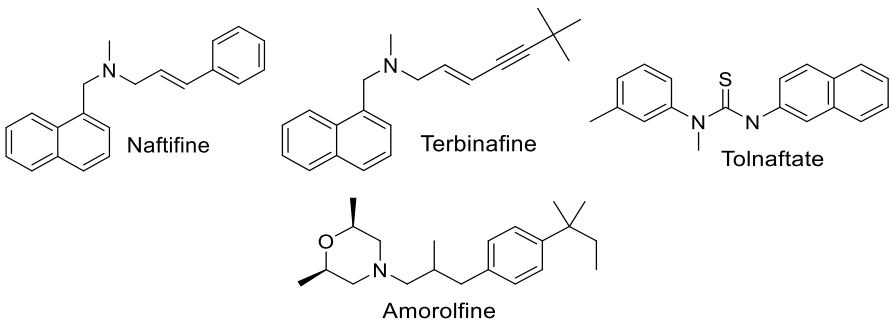

Figure 7 - Structures of antifungal inhibitors of ergosterol biosynthesis, allylamine – naftifine and terbinafine, thiocarbamate – tolnaftate and morpholine – amorolfine.

2.2. Antifungal drug resistance

In the past few decades, the frequency of microbial infections has increased dramatically. Besides, the treatment of these infections is increasingly complicated by the ability of microorganisms to develop resistance to antimicrobial agents.

Multidrug resistance (MDR) is defined as insensitivity or resistance of a microorganism to the administered antimicrobial medicines despite earlier sensitivity to it[38]. According to the World Health Organization (WHO)[39], these resistant microorganisms (such as bacteria, fungi, viruses, and parasites) are able to resist to action of antimicrobial drugs (like antibiotics, antifungals, antivirals, antimalarials, and anti-helminthic), which leads to ineffective treatment, resulting in persistent infections. Estimates suggest that each year, infections caused by MDR organisms result in about 25,000 deaths in European Union[40] and 23,000 deaths in the USA[41].

Antimicrobial drug resistance is conferred mostly because of acquisition of resistant mutations in microorganisms, although factors associated with antimicrobial usage, non-optimal prescriptions, incorrect dosage, and duration also contribute for antimicrobial resistance[42].

The resistance by microorganisms can essentially be acquired through three major mechanisms, namely, reducing the accumulation of the drug within the fungal cell, decreasing the affinity of the drug for its target, and modifications of metabolism to counterbalance the drug effect (**Table 1**). The extents of antifungal drug resistance vary for the different drug classes. Antifungal resistance to the polyenes, allylamines, and echinocandins is fairly limited, on the other hand, resistance to 5-FC and azoles is more common[20].

Table 1 - Target, mode of action, and fungal resistance mechanisms of the major antifungal drugs used in human therapy. Adapted from[20, 35].

Antifungal agent	Primary target (mode of action)	Mechanism of resistance
Azoles	Ergosterol biosynthesis (reduce ergosterol synthesis by inhibiting lanosterol 14α-demethylase (*ERG11*))	Efflux via ABC and MFS transporters, decrease of affinity in Erg11p by mutations, upregulation of *ERG11*, alterations in the ergosterol biosynthetic pathway
Echinocandins	Cell wall biosynthesis (reduce fungal cell wall glycan synthesis by inhibiting 1,3-β-glucan synthase)	Mutation in 1,3-β-glucan synthase

Antifungal agent	Primary target (mode of action)	Mechanism of resistance
Polyenes	Cell membrane ergosterol (bind to ergosterol and reduce integrity of cell membrane)	Absence of ergosterol, decrease of ergosterol content in cells
Fluorocytosine	RNA and DNA synthesis (antimetabolite interferes with nucleic acids synthesis)	Defect in cytosine permease, deficiency or lack of enzymes implicated in the metabolism of 5-FC, deregulation of the pyrimidine biosynthetic pathway
Allylamines	Ergosterol biosynthesis (reduces ergosterol synthesis by inhibiting squalene epoxidase; accumulation of toxic sterol intermediates)	Mutations in squalene epoxidase, efflux via ABC transporters,

2.3. Efflux-mediated antifungal resistance

Fungi drug-resistance or -insensitivity can be a result of the increase of the activity drug efflux pumps. These efflux pumps are transporter proteins that decrease the activity of conventional antimicrobial agents, by transferring them from within to the outside of the cell, which leads to a subsequent reduction in the intracellular accumulation of antimicrobials[42-43].

There are two main families of efflux pump proteins in fungi, the ATP-binding cassette (ABC) proteins and the major facilitator superfamily (MFS) transporters[44]. These two transports involve different mechanistic strategies to efflux drugs: while ABC proteins are primary active transporters that employ energy from the hydrolysis of adenosine 5'-triphosphate (ATP) to drive the efflux of drugs, those belonging to MFS are secondary active transporters that utilize the electrochemical gradient of protons across the plasma membrane to efflux substrates[45].

2.3.1. Fungal ATP-binding cassette transporters

The superfamily of ABC transporters is a large group of transmembrane proteins with more than 100 membrane transporters/channels that are involved in diverse functions[46-47]. These membrane transporters couple the energy released from ATP hydrolysis to the uptake and efflux, across of cells and organelles membranes, of a wide variety of substrates, including lipids, heavy metal ions, inorganic acids, glutathione conjugates, sugars, amino acids, peptides, secondary metabolites, and xenobiotics, such as drugs[48-49].

Structurally, the transporters belonging to ABC family contain two types of domain, hydrophobic transmembrane domains (TMD), normally containing six membrane-spanning α-helices, and cytoplasmic domains, also known as nucleotide binding domain (NBD), which are involved in ATP binding[48, 50-52].

The NBDs contain several highly conserved motifs, Walker A and Walker B motifs as well as the ABC signature motif which play a vital role in the hydrolysis of ATP to adenosine 5'-diphosphate (ADP) + phosphate (Pi) via an ATPase and energy collecting[53]. On the other hand, the TMDs are structurally diverse, and participate in translocation of substrate across the membrane[44, 53]. The general structure of the ABC transporters is evidenced in **Figure 8**.

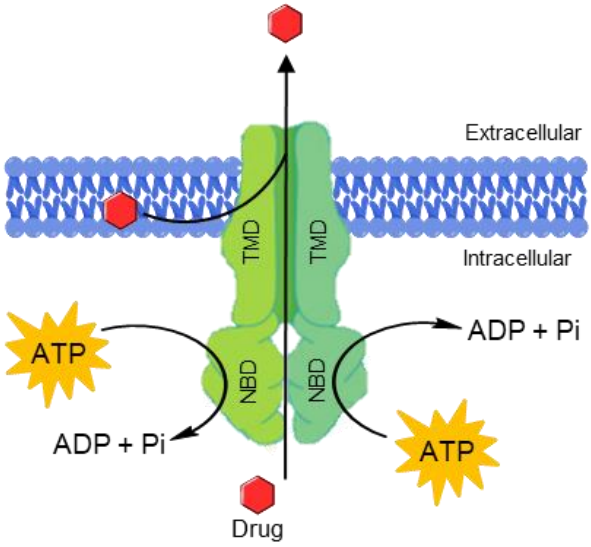

Figure 8 - Structure of ABC transporters.

Most fungal ABC proteins contain four domains, two NBDs (NBD1 and NBD2) and two TMDs (TMD1 and TMD2) and are referred to as “full-size” ABC transporters. In many organisms, there are “half-size” transporters consisting of one NBD and one TMD, and it is likely that these proteins dimerize to form active transporters[44]. The arrangement of the NBDs and TMDs within “full-size” ABC proteins varies between transporter subclass (**Figure 8**). Pleiotropic drug resistance (PDR), MDR, and multidrug resistance-associated protein (MRP) subfamilies, are the three main subfamilies of this family of carriers presents in *Saccharomyces cerevisiae*[20]. The domain arrangement in most MDR and MRP ABC protein is N-TMD1-NBD1-TMD2-NBD2-C, and for most PDR pumps the arrangement is reverse, N-NBD1-TMD1-NBD2-TMD2-C[54].

The subclass PDR is one of the largest families of ABC transporters in fungi[55]. *C. albicans* is predicted to have about 27 of ABC proteins, *C. glabrata* found to encode

approximately two-thirds that number (18), in the other hand, *A. fumigatus* (49) and *C. neoformans* (54) have a much larger numbers of ABC proteins[56].

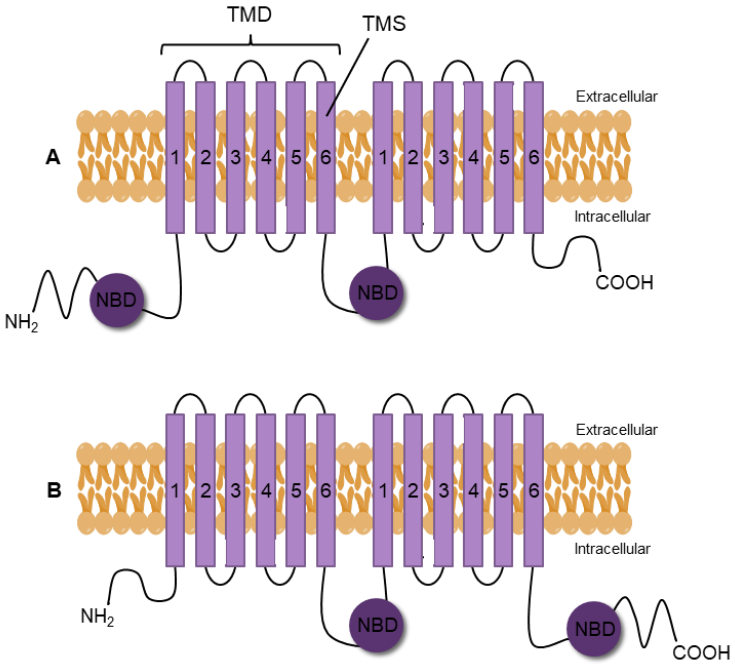

Figure 9 – Domain arrangements of ABC transporters, (**A**) (NBD-TMS_6)$_2$, (**B**) (TMS_6-NDB)$_2$. TMS, transmembrane segment.

This subfamily of fungal ABC proteins contains most of the transporters involved in antifungal drug resistance[20]. These PDR ABC transporters appear to share common features on both sides of the two TMDs that separate the intracellular from the extracellular space (**Figure 9**). The intracellular side contain a large N-terminal domain, NBD1, followed by two small intracellular loops (IL1 and IL2), a second large domain, NBD2, and another two small loops (IL-3 and IL-4). On the extracellular side these fungal PDR proteins appear to have four small extracellular loops (EL1, EL2, EL4, and EL5) and two large extracellular loops between TMS5 and TMS6 (EL3) and between TMS11 and TMS12 (EL6). These ELs contain residues and motifs highly conserved among PDR ABC transporters[20, 44].

Several transporters belonging to the PDR family that confer resistance to members of the antifungal class of azoles have been described. These transporters include the ABC transporters CDR1 and CDR2 (*Candida* drug resistance 1 and 2) in *C. albicans*; AFR1 in *C. neoformans*; ABC1 in *C. krusei*; and CgCDR1, PDH1 (also referred to as CgCDR2), and SNQ2 in *C. glabrata*[55].

2.3.2. Major facilitator superfamily

In addition to ABC transporters, a number of MFS transporters have also been demonstrated to be involved in MDR in fungi[57-58]. MFS proteins are capable of translocate substrates across membranes in response to electrochemical potential or function as drug:H^+ antiporter in microorganisms[59] (**Figure 10**).

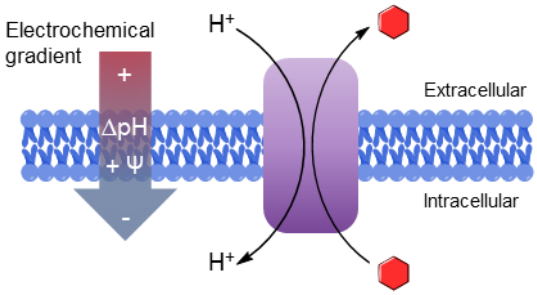

Figure 10 - Structure of MFS transporters.

The MFS transporters are smaller in size compared to the ABC transporters since they do not possess NBDs domains, but do contain TMS's that are thought to form the substrate channel. In fungi, there are two subfamilies of MFS transporters involved in drug efflux that are defined by the number of TMS within the TMD. The DHA1 subfamily (drug:H^+ antiporter 1) contains 12 TMS and the DHA2 subfamily 14 TMS[44].

The number of genes encoding MFS transporters in fungi varies greatly between species with ten in *A. gossypii* and 149–174 in *C. neoformans*. Among these transporters, only a subset is involved in drug efflux[44]. *CaMDR1* (formally *BEN*^{r}), a DHA1 MFS transporter, was the first MFS transporter gene to be characterized from a pathogenic fungus. This gene was originally described to encode resistance to benomyl and methotrexate on *S. cerevisiae*. The resistance conferred by this DHA1 MFS transporter, unlike the ABC proteins, is specific for FLC among the azoles. Structural and functional analyses of CaMdr1p have indicated that amino acid residues located in TMS5 are important for drug:H^+ translocation[20]. Another multidrug transporter in the MFS class is encoded by FLU1 in *C. albicans*. Like CaMDR1, this resistance did not extend to the other azoles. Its disruption had little effect on FLC susceptibility, indicating that FLU1 expression is not associated with azole resistance in clinical isolates[20].

Therefore, despite the involvement of MFS genes in the azole resistance of certain clinical *Candida* isolates, there is, in general, a much stronger association between azole resistance and the expression of PDR ABC genes. Furthermore, when the expression of efflux pumps in clinical *C. albicans* isolates resistant to azoles was analyzed it was found that ABC pumps were more often overexpressed than MFS pumps[20, 44].

2.4. Approaches for overcoming efflux-mediated antifungal drug resistance

An ideal antifungal agent, in addition to meeting several pharmacological requirements, such as having a broad spectrum of activity against a variety of fungal species, be fungicidal rather than fungistatic, be directed at a specific fungal target have minimal side effects or toxicity, would not be susceptible to the development of resistance due to efflux mechanisms. There are several strategies to overcome efflux-mediated antifungal drug resistance (**Figure 11**).

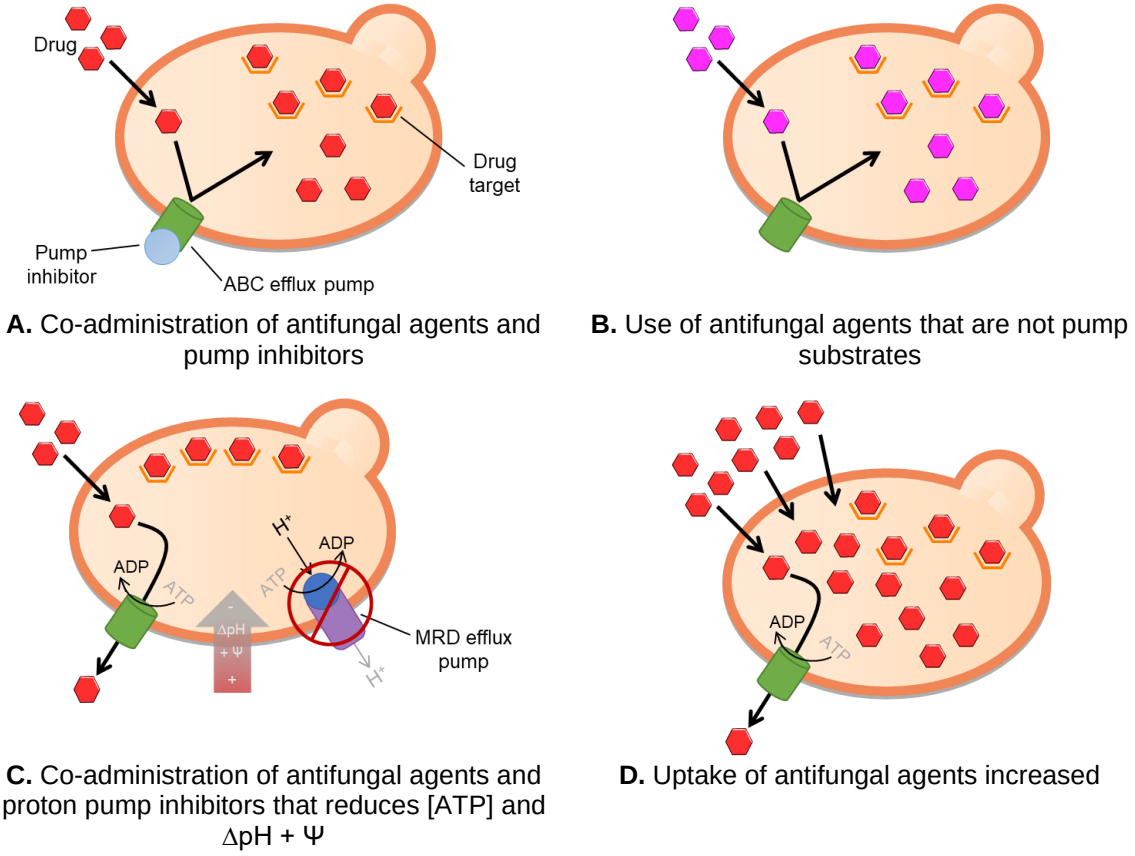

A. Co-administration of antifungal agents and pump inhibitors

B. Use of antifungal agents that are not pump substrates

C. Co-administration of antifungal agents and proton pump inhibitors that reduces [ATP] and ΔpH + Ψ

D. Uptake of antifungal agents increased

Figure 11 - Strategies to circumvent efflux-mediated antifungal drug resistance. ABC, ATP-binding cassette superfamily; MDR, Multidrug resistance pump; ATP, Adenosine triphosphate; ADP, adenosine diphosphate. Adapted from[20].

One of the strategies to overcome efflux pump-mediated antifungal drug resistance is to inhibit the pumps and chemosensitizer resistant strains to antifungals (**Figure 11A**). Strategies such as the use of antifungals that are not substrates of drug transporters (e.g. polyenes and echinocandins) (**Figure 11B**), or by depleting cells of the energy required for drug efflux by inhibiting the plasma membrane H^+ ATPase (for ABC pumps) or depleting the electrochemical potential of the plasma membrane (for MFS transporters)[60] (**Figure 11C**) have also been described in the literature. Other approach could be to increase uptake rather than decrease efflux of drugs (**Figure 11D**).

Efflux pump inhibition

The concept of reverting drug resistance through the inhibition of efflux pumps is not new. A major impetus for this work has come from cancer research, because the human drug efflux pumps are important mediators of resistance of tumor cells to chemotherapeutic agents[20, 44]. Ever since the detection of human ABC protein P-glycoprotein (P-gp) in over 400 human cancers[61], identifying and developing P-gp inhibitors has been a principal focus area in drug discovery[62]. Indeed, three generations of P-gp inhibitors entered clinical trials. The first-generation inhibitors included compounds pharmacologically active, which were developed and are in clinical use for other indications, but that also demonstrated to be P-gp inhibitors (e.g. verapamil, cyclosporine A and quinine)[63]. Despite potent *in vitro* activity this class of compounds exhibited toxicity *in vivo*[63]. Second-generation of inhibitors includes compounds resulting from structural modifications of the first-generation members to target specific MDR transporters. These compounds, such as valspodar had improved bioavailability and less toxicity, but demonstrated off-target effects and lacked significant efficacy in clinical trials[64]. The third generation of P-gp inhibitors was developed by using quantitative structure-activity relationships (QSAR) and combinatorial chemistry to improve potency and specificity. Drugs zosuquidar, elacridar, laniquidar, tariquidar and CBT-1 are some of the most studied inhibitors of the third generation of P-gp inhibitors. A problem in this generation of P-gp inhibitors is that unexpected toxic effects were still observed in clinical assays[62, 64].

A class of studied molecules that has been found to exhibit P-gp modulation activities is the thioxanthone[1]. In fact, previous studies have already reported the ability of aminated thioxanthones to act as inhibitors of P-gp (**Figure 12**)[18].

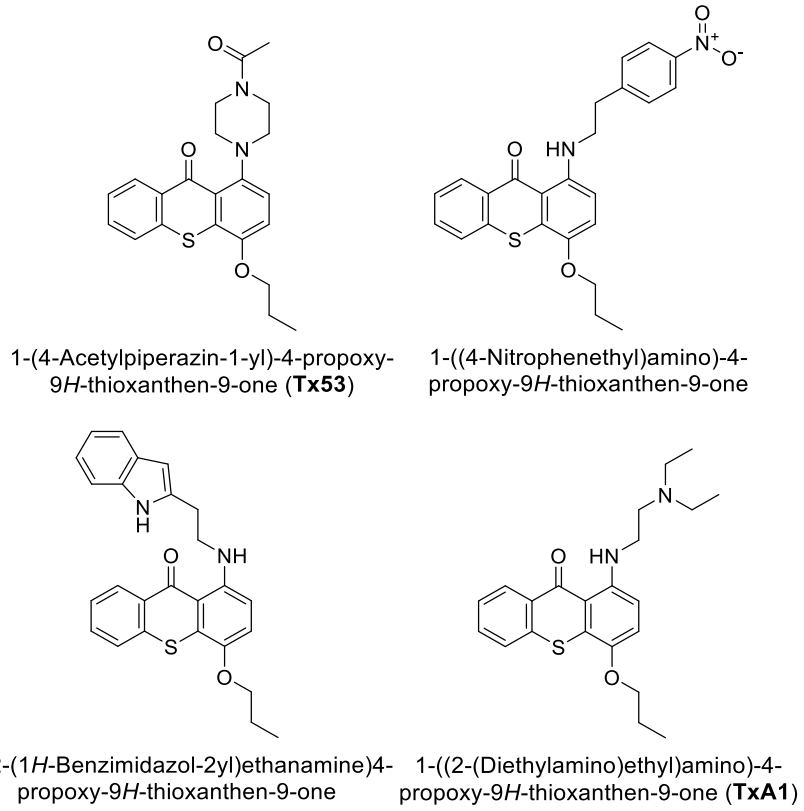

Figure 12 - Examples of aminated thioxanthones inhibitors of P-gp[18].

The approach of inhibiting transporters in order to overcome drug resistance is also being applied in some bacterial and fungal pathogens[65-66] being recently revised by the group[50]. Such strategy can also be applied to the development of fungal ABC pump inhibitors. Heterologous expression of efflux pumps in the model yeast *S. cerevisiae* has been used to screen for compounds that inhibit the transporters and thus chemosensitize cells to existing effective antifungal drugs[20]. A variety of medium-throughput and high-throughput screens have been used to identify fungal efflux pump inhibitors. Screens to identify inhibitors of fungal efflux pumps can be based on yeast growth measurements that demonstrate the reversal of fungal resistance to a pump substrate such as the azoles (growth chemosensitization assay) or can utilize the fluorescent properties of certain pump substrates such as rhodamine 6G, nile red or diS-C3[44].

3. Susceptibility testing

Antifungal susceptibility testing remains an area of intense interest. Susceptibility testing methods are available to detect antifungal resistance, through epidemiological studies, and to determine the best treatment for a specific fungus; furthermore, antifungal susceptibility testing can be used for drug discovery[67-68]. These tests determine fungal growth in the presence of different concentrations of antifungal compounds.

The methods to evaluate antifungal susceptibility can be divided in semi-quantitative, which enables the categorization as susceptible, intermediate/dose dependent or resistant; or a quantitative, which determine the minimal inhibitory concentrations (MIC), the minimum concentration of antimicrobial agent that cause a specific reduction in visible growth of a microorganism.

There are several types of antifungal susceptibility testing procedures, including broth macrodilution and microdilution, agar diffusion, disk diffusion, and Etest[69]. Among all these methods, microdilution methods are the gold standard or reference techniques[67].

The European Committee on Antibiotic Susceptibility Testing (EUCAST) and Clinical and Laboratory Standards Institute (CLSI) have developed standardized methods for the performance of antifungal susceptibility. In 1985, CLSI, formerly known as the US National Committee for Clinical and Laboratory Standards (NCCLS), formed a subcommittee on Antifungal Susceptibility Testing, which, in 1997, published the document M27A “Reference Method for Broth Dilution Antifungal Susceptibility Testing of Yeast; Approved Standard”[70]. This document defined reference strains with ranges of MIC and breakpoints for some antifungal agents and their action against several yeasts such as *Candida* and *Cryptococcus*. Since then, several updates have been published, the current one having been approved in 2008[71]. For filamentous fungi, the document M38-A2: "Reference Method for Broth Dilution Antifungal Susceptibility Testing of Filamentous Fungi; Approved Standard" published in 2008, is the currently accepted one[72]. These methods specify inoculum size and preparation, test medium, incubation time, temperature, and breakpoints reading.

In this dissertation, the evaluation of antifungal susceptibility of yeast fungi to synthesize compounds was performed using the plate microdilution method according to CLSI standards, M27-A3.

CHAPTER II:
AIMS

II. Aims

The main purpose of this dissertation is the development of thioxanthones with potential antifungal synergistic effect.

Thioxanthones are an important class of molecules showing interesting biological properties, including P-glycoprotein efflux pump inhibition as previously mentioned[73]. Overexpression of efflux pumps is broadly recognized as major component of resistance also to many classes of antimicrobials, and thus, these pumps can be considered potential targets to overcome this resistance[21]. This work has already started in our group.

Considering the fact that thioxanthones are considered privileged structures, this scaffold was selected for further studies within the scope of this dissertation in finding new efflux pump inhibitors to overcome antifungal multidrug resistance and/or new antifungals.

Within a broader project (PTDC/SAU-PUB/28736/2017) to discover efflux pump inhibitors (EPIs) to revert antibacterial and antifungal drugs resistance, and inspired in the previously known P-gp inhibitors, a series of new thioxanthone derivatives was designed by performing docking studies on several bacterial efflux pumps. Among the designed molecules, a series of molecules was selected to be the target compounds of this dissertation which contained: i) aminated motifs that were previously found in already described EPIs or antifungal agents, or ii) halogenated thioxanthones. This last selection was related with the recent discovery from our research group of chlorinated xanthones as interesting antifungal agents.

The specific aims of this dissertation were:

i) to synthesize a series of new aminated thioxanthones by coupling reactions of a chlorinated thioxanthone with aminated building blocks;

ii) to improve the Ullmann coupling reaction by changing the started material to a brominated thioxanthone

iii) to characterize through spectroscopic techniques the structure of the synthesized derivatives;

iv) to screen the antifungal activities of the synthetized compounds, and particularly their ability to act synergistically with azoles against *Candida* spp.

CHAPTER III:
Results and Discussion

III. Results and Discussion

PART 1 – CHEMISTRY

1.1. Synthesis of thioxanthonic derivatives

Accordingly to our aims, the synthesis and characterization of new 1-amino thioxanthonic derivatives, using 1-halogenated-4-propoxy-9*H*-thioxanthen-9-one (**TxCl** and **TxBr**) as chemical substrate (**Figure 13**) was planned.

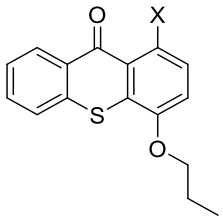

TxCl: X = Cl
TxBr: X = Br

Figure 13 - Chemical structure of the thioxanthone chemical substrates.

In summary, the synthesis of five new derivatives (**Tx 2**, **Tx 4**, **Tx 5**, **Tx 7**, and **Tx 11**) was accomplished by a copper-catalyzed Ullmann reaction type C(1)-N coupling between the thioxanthone derivative 1-halogenated-4-propoxy-9*H*-thioxanthen-9-one (**TxCl** and **TxBr**) with primary or a secondary amines (**A 2**, **A 4**, **A 5**, **A 7**, and **A 11**) (**Table 2**). Along with the new aminated thioxanthones, **Tx 4** and **11**, three new thiochromene quinazolines derivatives, **Tx 2**, **5** and **7** were unexpectedly synthesized (**Table 2**).

The reactions were accomplished by a nucleophilic aromatic substitution of the chloride or the bromide in position C-1 of the thioxanthone scaffold by the amine, affording the thioxanthonic derivatives **Tx 4** and **Tx 11** followed by an intramolecular dehydrative cyclization for derivatives **Tx 2**, **Tx 5**, and **Tx 7**.

Table 2 - Summary of the obtained derivatives in this dissertation.

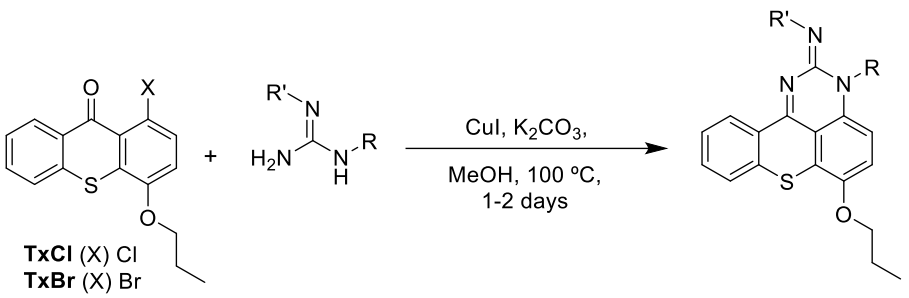

TxCl (X) Cl
TxBr (X) Br

Thioxanthone starting material	Amine starting material	Isolated product
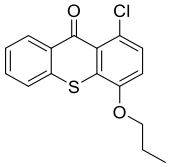	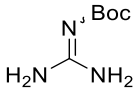	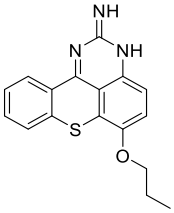
TxCl	**A 2**	**Tx 2**
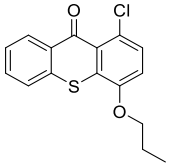	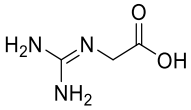	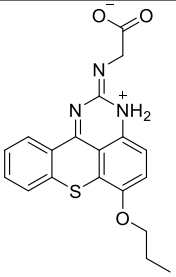
TxCl	**A 5**	**Tx 5**
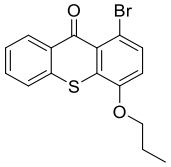	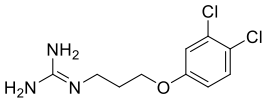	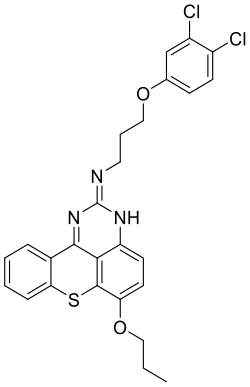
TxBr	**A 7**	**Tx 7**

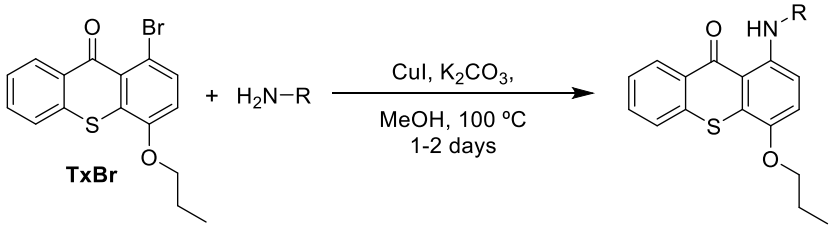

TxBr

Thioxanthone starting material	Amine starting material	Isolated product

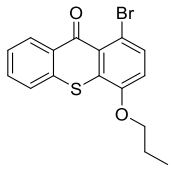	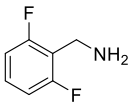	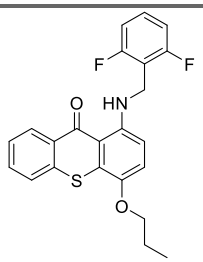
TxBr	**A 4**	**Tx 4**
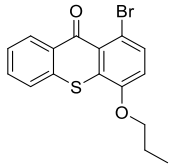	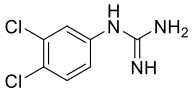	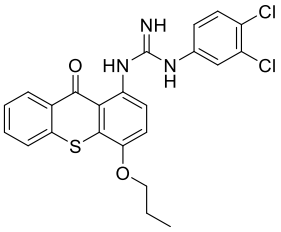
TxBr	**A 11**	**Tx 11**

The mechanistic proposal for the synthesis of these derivatives is exemplified for compounds **Tx 4** and **Tx 5** in **Scheme 1**.

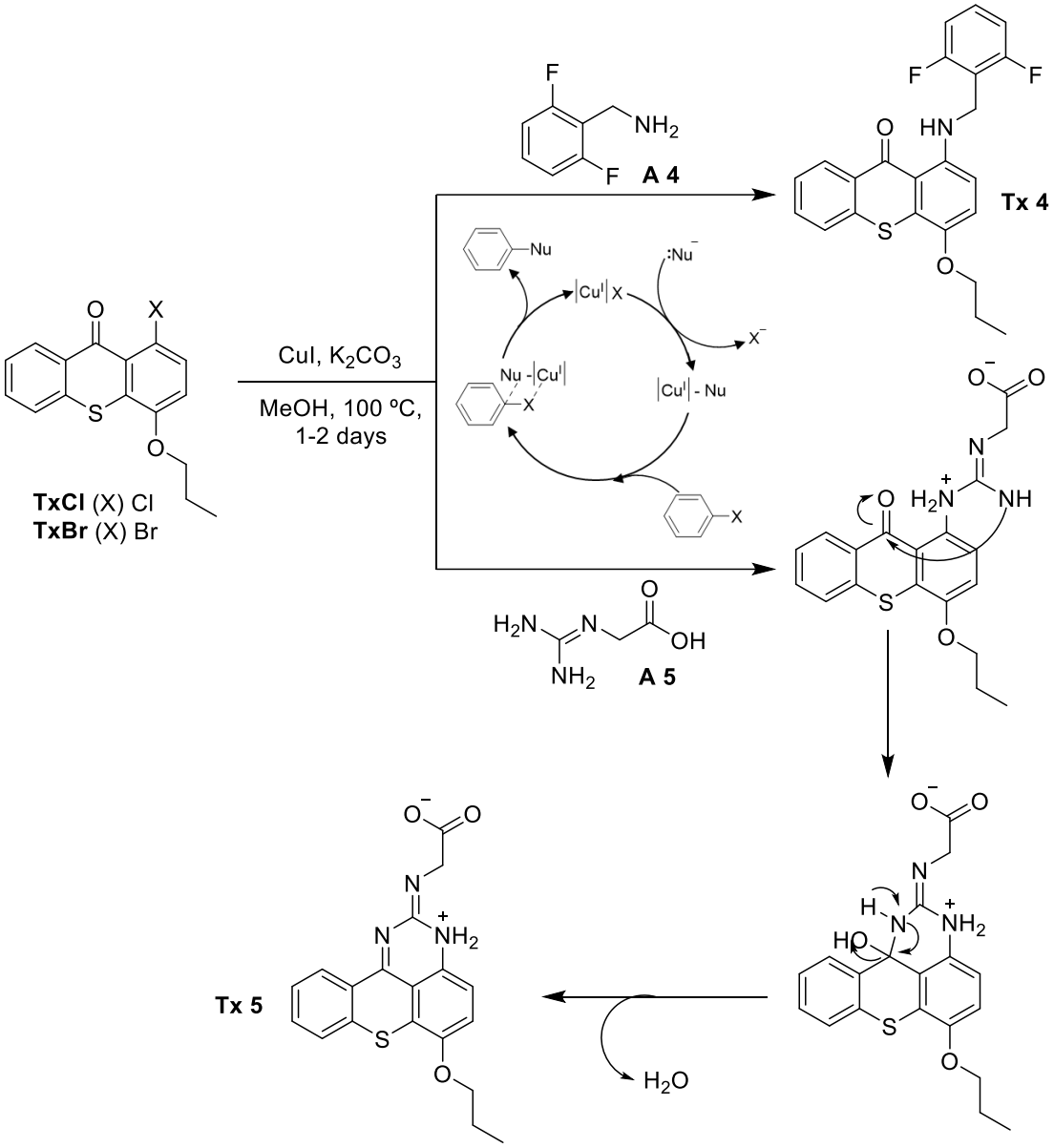

Scheme 1 - Representative reactions mechanism proposal for the reactions undertaken in this dissertation.

1.1.1. Synthesis of aminated derivatives Tx 2 and Tx 5

The conditions used for the synthesis of compounds 6-propoxythiochromeno[4,3,2-*de*]quinazolin-2(3*H*)-imine (**Tx 2**) and 2-((6-propoxythiochromeno[4,3,2-*de*]quinazolin-3-ium-2(3*H*)-ylidene)amino)acetate (**Tx 5**) were based on previous described procedures[3]. Both syntheses were performed in alkaline medium, provided by the addition of K_2CO_3, in a closed vessel, mixing the appropriate amine (**A 2** and **5**), in excess, with 1-chloro-4-propoxy-9*H*-thioxanthen-9-one (**TxCl**), CuI in catalytic amounts in methanol. The reactions were carried out at 100 °C for 1-2 days, without stirring.

The reactions progress was monitored by thin layer chromatography (TLC) analysis using chloroform/acetone, 9:1 (v/v) as mobile phase and observed under ultraviolet (UV)

light at 254 and 365 nm. After completing the reaction, they were first filtered in order to eliminate the CuI. A chemical liquid-liquid extraction with HCl solution was performed in the reactions to remove most of the acidic/neutral organic impurities. Then, the amines were regenerated with NaOH, extracted and the extract was further subjected to a flash chromatography. These purification processes were insufficient to isolate pure thioxanthonic derivatives. Thus, thioxanthones **Tx 2** and **Tx 5** were further purified by solid phase extraction (SPE) with a cation exchange cartridge to eliminate remaining impurities.

Unexpectedly, the target compounds were not obtained; instead of the designed aminated thioxanthones planned, two thiochromene quinazolines derivatives, **Tx 2** and **Tx 5** were obtained in these conditions.

Although not for these compounds, the formation of this scaffold was previously described in the literature, through a tandem copper-catalyzed Ullman C-N coupling and a dehydrative cyclization[74]. This synthetic approach involves initial Ullmann-type C-N coupling followed by intramolecular dehydrative cyclization between **TxCl** and primary amine **A 2** and **5** (**Scheme 2**).

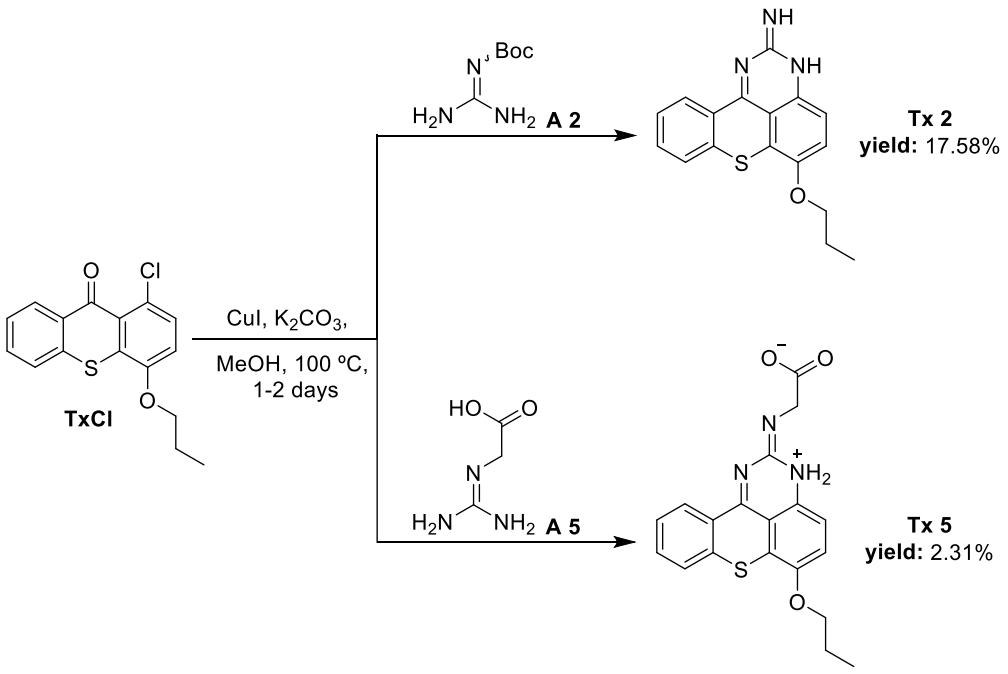

Scheme 2 - General scheme of the synthesis of thiochromeno[4,3,2-*de*]quinazolines. Boc – *tert*-butoxycarbonyl.

The obtained isolated yields were very low (**Scheme 2**). This was a consequence of the formation of a secondary product, a methoxylated derivative of the thioxanthone (**TxOMe**) (**Figure 14**), corresponding to the competition of C-O cross coupling. This byproduct was identified by TLC by the comparison with a standard previously synthesized and characterized, using the same reaction conditions[1]. Besides **TxOMe**, other byproducts

were detected, making the purification steps of the desired thioxanthone quite different and time consuming.

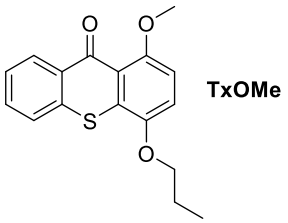

Figure 14 - Chemical structure of the secondary product 1-methoxy-4-propoxy-9*H*-thioxanthen-9-one (**TxOMe**).

The same reaction conditions failed to produce the desired amino derivatives when amines **A 1** and **A 3** (**Figure 16**) were used building blocks.

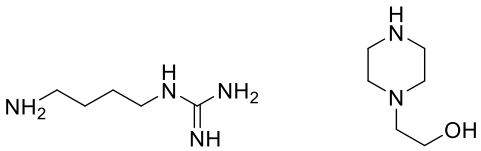

A 1 **A 3**

Figure 15 - Chemical structure of the amines used as building blocks.

In order to afford these two amino derivatives, several purification steps were performed, such as chemical liquid-liquid extraction, flash column chromatography and preparative TLC. However, despite efforts to purify, the desired aminated thioxanthones were not isolated.

1.1.2. Halogen exchange reaction

In order to improve the yields of the N-C cross-coupling reactions, the exchange of chlorine for bromine was attempted, since aryl bromides are more reactive than aryl chlorides[75].

The synthesis of brominated thioxanthone as starting material for the synthesis of the 1-amino-halogenated thioxanthonic derivatives was achieved by nucleophilic aromatic substitution based on previous described procedures[76].

The chlorinated thioxanthone **TxCl** was used as starting material for the synthesis of the1-bromo-4-propoxy-9*H*-thioxanthen-9-one (**TxBr**). Chlorine exchange by bromine was performed using potassium bromide (KBr) in excess (1:5) in the presence of phosphoric acid. The reaction was performed under reflux (200 °C) using nitrobenzene ($PhNO_2$) as solvent (**Scheme 3**). After 24 hours, the reaction mixture was washed with water and extracted with dichloromethane and then this procedure was repeated one more time.

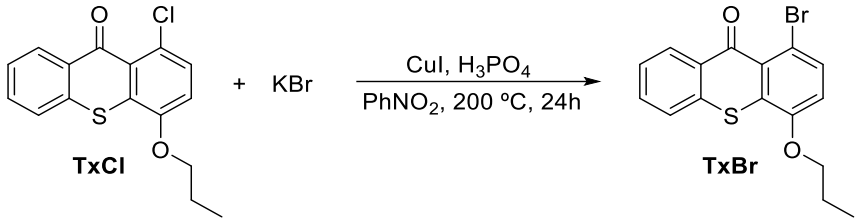

Scheme 3 - General reaction of exchange of chlorine for bromine.

The reaction progress was monitored by TLC analysis using dichloromethane/acetone, 9:1 (v/v) as mobile phase. The UV light at 254 and 365 nm and a solution of sulfuric acid in ethanol (activated by heat) were used for visualization of chromatograms.

After completing this procedure, in order to afford the brominated thioxanthone, successive purifications were carried out. Firstly, a flash chromatography using *n*-hexane/ethyl acetate as eluent was performed with the extract to eliminate the solvent $PhNO_2$. However, no pure fractions were obtained, and therefore, the fractions that contained the same chromatographic profile were joined. Subsequently, the fractions with the desired compound were subjected to a further purification process by crystallization from methanol.

As expected, this synthetic approach yielded the desirable product; however, the obtained yield (53%) was lower than the previously described for other scaffolds.

1.1.3. Synthesis of amino-halogenated derivatives Tx 4, Tx 7, and Tx 11

The brominated thioxanthone **TxBr** was used as started material for the synthesis of the amino-halogenated thioxanthones **Tx 4**, **Tx 7**, and **Tx 11**, by copper catalyzed aromatic nucleophilic substitution reaction. The reaction conditions used in the synthesis of these compounds were similar to those described in section 1.1.1. The synthesis was performed with the amine in excess (two equivalents of amine, **A 4**, **7** and **11**) and thioxanthone **TxBr** as limiting reagent, CuI in catalytic amounts at 100 ºC in a closed vessel for 1-2 days.

The reactions progress was monitored by TLC analysis using chloroform/acetone, 9:1 (v/v) as mobile phase and observed under UV light at 254 and 365 nm.

The work-up of the reactions followed a general procedure. After finishing the reaction, the crude material was first filtered. Then, a liquid-liquid extraction with chloroform was performed in order to remove inorganic impurities. The extract was further subjected to a flash chromatography to eliminate remaining impurities (**TxOMe** and other compounds with similar chromatographic behavior).

This sequence of purifications was successful for the purification of thioxanthonic derivative **4**. However, they were insufficient to isolate pure aminated thioxanthones **7** and **11**. For these two thioxanthonic derivatives, a further purification process by preparative TLC was needed.

This synthetic approach yielded the desirable products 1-((2,6-difluorobenzyl)amino)-4-propoxy-9*H*-thioxanthen-9-one (**Tx 4)** and 1-(3,4-dichlorophenyl)-3-(9-oxo-4-propoxy-9*H*-thioxanthen-1-yl)guanidine (**Tx 11**), as occurred for similar compounds in a previous work[18]. However, the thiochromene quinazoline *N*-(3-(3,4-dichlorophenoxy)propyl)-6-propoxythiochromeno[4,3,2-*de*]quinazolin-2(3*H*)-imine (**Tx 7**) was obtained similarly as with **Tx 2** and **Tx 5** (**Scheme 4**).

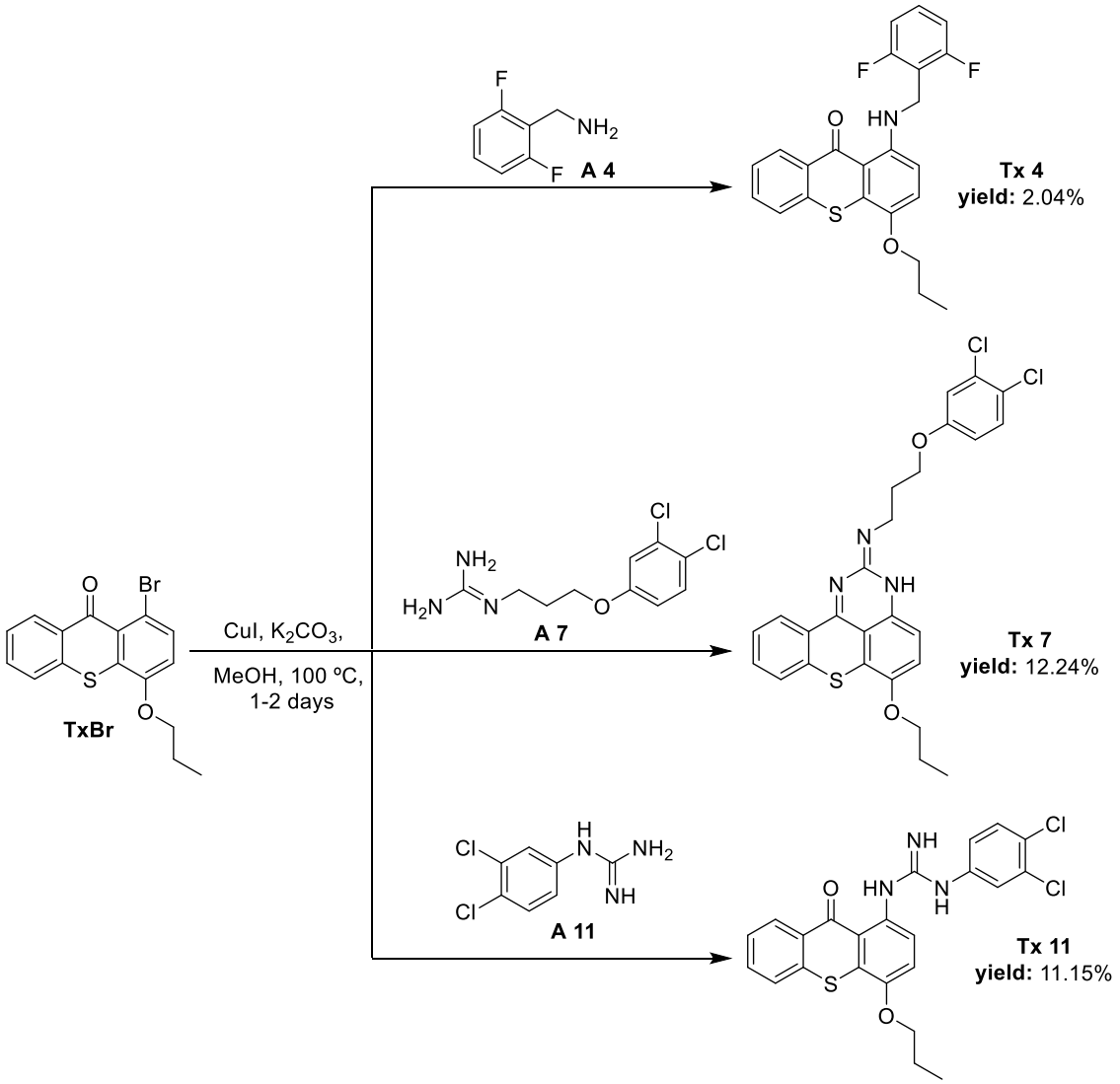

Scheme 4 - General scheme of the synthesis of compounds **Tx 4**, **Tx 7** and **Tx 11**.

The yields of these reactions were very low ranging from 12 to 2 % (**Scheme 4**). As previously mentioned, these low yields could be explained by the fact that these reactions have been incomplete, and due the formation of the secondary product **TxOMe**.

Despite this reaction conditions work to produce compounds **Tx 4**, **7** and **11**, this synthetic approach failed to produce the desired amino derivatives when halogenated amines **A 6** and **A 8** (**Figure 16**) were used building blocks.

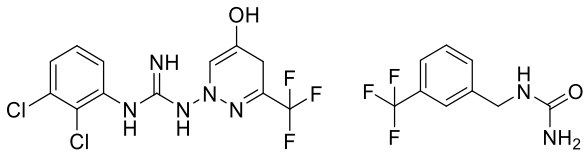

A 6 **A 8**

Figure 16 - Chemical structure of the halogenated amines used as building blocks.

Although a red spot, characteristic of thioxanthones aminated at C-1, could be observed in the TLC at day light after 24 hours of reaction, successive attempts of purification were unsuccessful in the isolation of the pure compounds, mostly due to their presence in vestigial amounts.

In order to improve the synthesis of amino-halogenated thioxanthones, several parameters concerning reaction conditions were investigated including the addition of the *trans-N,N'*-dimethylcyclohexane-1,2-diamine (DMCHDA) as the ligand to reduce the amount of undesirable substitution product (**TxOMe**). Since microwave-promoted synthesis is a crescent interest in N-C cross-coupling reaction, the heating source was also modified. Additionally, the solvent was change to *N*-methyl-2-pyrrolidone (NMP), an aprotic, alkaline solvent (**Scheme 5**). To our disappointment, it has been found that these reaction conditions did not give the desired amino-halogenated thioxanthones presumably because of the steric hindrance of the amines.

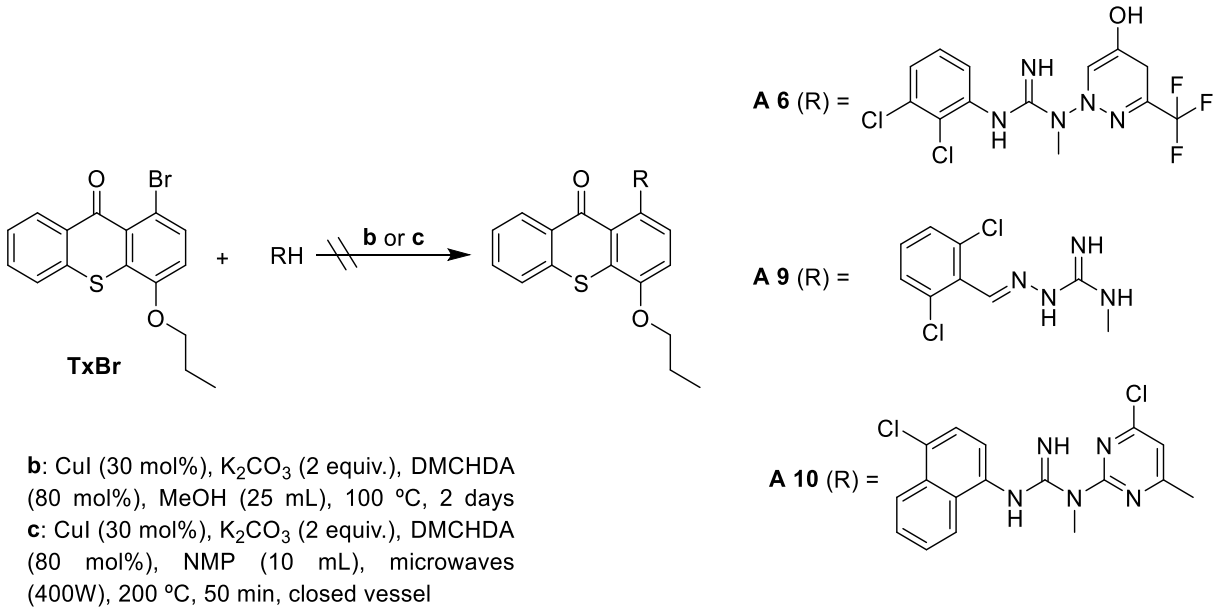

Scheme 5 - General conditions employed for the synthesis of amino-halogenated thioxanthones.

1.2. Determination of thioxanthones purity

The purity of synthesized thioxanthones **Tx 2**, **4**, **5** and **7** was determined by high performance liquid chromatography with diode-array detection (HPLC-DAD) analysis, using a C18 (250 × 4.6mm) stationary phase and a mixture of methanol:water (trifluoroacetic acid 0.1%) (80:20 v/v) as mobile phase, and the results obtained are presented in **Table 3**.

Table 3 - HPLC retention time and purity of the synthesized compounds.

Compound	Retention time (min)	Purity (%)
Tx 2	6.5	99.9
Tx 4	10.7	98.5
Tx 5	6.5	98.3
Tx 7	26.7	99.1

Flow rate =1 mL/min

1.3. Structure elucidation

The structure elucidation of the new synthesized brominated thioxanthone as well as the amino thioxanthonic derivatives was established for the first time by infrared (IR) and nuclear magnetic resonance (NMR) techniques. In this section, it will be presented IR, ^{1}H and ^{13}C NMR data for the new thioxanthonic derivatives.

1.3.1. IR spectroscopy data

The IR data of the synthesized thioxanthonic derivatives are presented in **Table 4**.

Table 4 - IR data of the synthesized thioxanthonic derivatives.

Compound	Group	Vmax (cm^{-1})
Tx 2	N-H	3297
	C=N	3157, 1640
	C-H	2963
	C-C	1569, 1558, 1453
	C-N	1261
	C-O	1231, 1064
Tx 5	O-H	3461
	N-H	3297
	C=N	3157, 1638
	C-H	2962, 2919, 2850
	C=O	1608
	C-C	1545, 1501, 1453
	C-N	1260
	C-O	1232, 1063
TxBr	C-H	2960, 2926, 2874
	C=O	1637
	C-C	1580, 1549, 1459
	C-O	1253, 1052
Tx 4	N-H	3270
	C-H	2960, 2924, 2849
	C=O	1618
	C-C	1594, 1560, 1468
	C-N	1274
	C-O	1231, 1050
Tx 7	N-H	3263
	C=N	3158, 1647
	C-H	2924, 2853
	C-C	1556, 1533, 1475
	C-N	1263
	C-O	1228, 1073
Tx 11	N-H	3258
	C-H	2960, 2922, 2850
	C=O	1610
	C-C	1570, 1553, 1508, 1466
	C-N	1263
	C-O	1227, 1076

The IR data for thiochromene quinazolines **Tx 2**, **Tx 5** and **Tx 7** indicates the presence of, bands corresponding to the C=N (1638–1647 and 3157–3158cm^{-1}), as well as, bands characteristic of C-N bond (1260–1263 cm^{-1}) and N-H bond (3263–3297 cm^{-1}). Additionally, the IR data indicate the presence of absorption bands corresponding to C-O (1060–1073 and 1224–1228 cm^{-1}), associated with the ether group of carbon 4, and aromatic C-C (1453–1569 cm^{-1}) groups. Additional bands corresponding to the C=O bond at 1608 cm^{-1} and to O-H bond (3461 cm^{-1}) were observed in IR spectrum of **Tx 5**.

The IR data for brominated thioxanthone **TxBr** indicates the presence of, a band corresponding to the C=O at 1637 cm^{-1}, as well as, bands corresponding to the C=C at aromatic bond typical from the thioxanthonic scaffold at 1580, 1549 and 1459 cm^{-1}. It is also important to highlight the presence of absorption bands corresponding to C-O (1253 and 1052 cm^{-1}), associated with the carbonyl ether group of aliphatic chain of carbon 4. Additional bands corresponding to the aromatic carbons (C-C bonds: 1459–1594 cm^{-1}), typical of thioxanthonic compounds, could be observed in IR spectrum. For the amino thioxanthones **Tx 4** and **Tx 11**, a similarity of IR spectrum profile was observed when compared to **TxBr**.

Comparing the IR spectrum of the aminated thioxanthones with **TxBr**, the detection of new bands corresponding to C-N (1263–1274 cm^{-1}) and N-H (3263–3272 cm^{-1}) bonds indicated that the binding of the amine building blocks to the thioxanthone scaffold was successfully accomplished. Moreover, considering the thioxanthonic scaffold, the IR data indicate the presence of an absorption band corresponding to C=O (1617–1618 cm^{-1}) and two absorption bands corresponding to C-O (1050–1078 and 1227–1231 cm^{-1}), as well as, bands corresponding to the C-C at aromatic bonds (1475–1594 cm^{-1}) typical from the thioxanthonic scaffold.

1.3.2. ^{1}H NMR data

The data corresponding to the ^{1}H NMR of synthesized compounds **Tx 2**, **4**, **5**, **7** and **11** are represented in **Tables 5–7**.

1.3.2.1. ^{1}H NMR for aminated derivatives Tx 2 and Tx 5

The ^{1}H NMR spectra of thiochromene quinazolines **Tx 2** and **Tx 5** exhibited the presence of signals corresponding to six aromatic protons H-2, H-3, H-5, H-6, H-7, and H-8 (δ_H values ranging from 7.2 to 8.8 ppm) of the precursor thioxanthone scaffold. The highest chemical shift value attributed to proton H-8 is due to the mesomeric and anisotropic effect of the imine group (C-9) that contributes to an electronic deprotection of this proton.

These spectra also revealed the presence of three signals corresponding to protons of the propoxy group H-a, H-b and H-c (δ_H values between 1.0 and 4.1 ppm).

For thiochromene quinazoline **Tx 2**, the absence of the signals corresponding to *tert*-butyloxycarbonyl group (*Boc*) of the aminated chain **A 2**, revealed that deprotection occurred with the reaction conditions used. In the case of the ^{1}H NMR spectrum of **Tx 5**, one singlet at δ_H 2.17 ppm was also observed, confirming the presence of hydrogen atoms on H-2' of the aminated chain; however, the signal corresponding to the OH of the carboxylic acid could not be observed.

The data corresponding to the ^{1}H NMR of **Tx 2** and **Tx 5** is represented in **Table 5**.

Table 5 - ^{1}H NMR data* for **Tx 2** and **Tx 5**.

	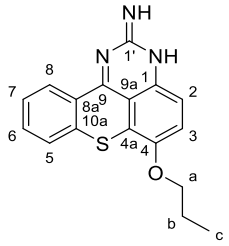 **Tx 2**		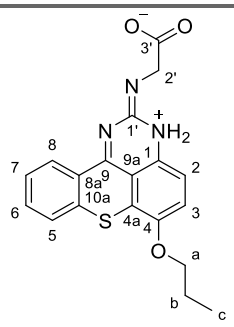 **Tx 5**
	δ_H		**δ_H**
H-8	8.71, 1H, dd, *J* = 8.2 and 0.9	**H-8**	8.80, 1H, dt, *J* = 8.0 and 1.1
H-6	7.60, 3H, m	**H-6**	7.42, 5H, m
H-5		**H-5**	
H-3		**H-7**	
H-7	7.46, 1H, ddd, *J* = 8.2, 6.6 and 1.7	**H-2**	
H-2	7.22,1H, d, *J* = 9.1	**H-3**	
NH	6.65, 2H, brs	**NH**	5.22, 2H, brs
H-a	4.13, 2H, t, *J* = 6.4	**H-a**	4.13, 2H, t, *J* = 6.4
H-b	1.78, 2H, st, *J* = 7.4	**H-2'**	2.17, 2H, s
H-c	1.05, 3H, t, J = 7.4	**H-b**	1.91, 2H, st, *J* = 7.4
		H-c	1.13, 3H, t, *J* = 7.4

*Values in ppm (δ_H) relative to $(CH_3)_4Si$ as an internal reference. *J* values are in Hz.

1.3.2.2. ^{1}H NMR for TxBr

The ^{1}H NMR spectrum of **TxBr** shows the presence of the signals corresponding to the six aromatic protons, namely H-2, H3, H-5, H-6, H-7, and H-8, with a range of chemical shifts between 6.89 and 8.45 ppm. The aromatic proton most deshielded is proton H-8. The mesomeric effect of the carbonyl group (C-9) contributes to an electronic deprotection of the *ortho* (H-8) and the *para* (H-6) positions of the aromatic ring. The magnetic anisotropy

of the carbonyl group (C-9) deshields preferentially proton H-8, which explains the highest chemical shift for the signal of proton H-8.

Concerning the signals of the aliphatic chain at C-4, the chemical shifts of H-a, H-b and H-c were comprised between 1.16 and 4.10 ppm.

The data corresponding to the ^{1}H NMR of **TxBr** is represented in **Table 6**.

Table 6 - ^{1}H NMR data* for **TxBr**.

	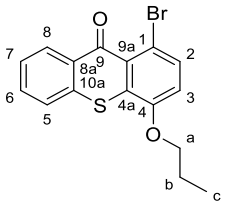 **TxBr**
	δ_H
H-8	8.45, 1H, dd, *J* = 8.1 and 0.8
H-2	7.66, 1H, d, J = 8.6
H-6	7.58, 2H, m
H-5	
H-7	7.46, 1H, ddd, *J* = 8.1, 5.4, and 2.8
H-3	6.89, 1H, d, *J* = 8.6
H-a	4.11, 2H, t, *J* = 6.4
H-b	1.94, 2H, st, *J* = 7.4
H-c	1.16, 3H, t, *J* = 7.4

*Values in ppm (δ_H) relative to $(CH_3)_4Si$ as an internal reference. *J* values are in Hz.

1.3.2.3. ^{1}H NMR for amino-halogenated derivatives Tx 4, Tx 7 and Tx 11

The ^{1}H NMR spectra of the three amino-halogenated derivatives showed a similarity with the respective starting material, **TxBr**, particularly in the chemical shifts of the signals corresponding to the aromatic protons H-2, H-3, H-5, H-6, H-7, and H-8 (δ_H values between 8.5 and 8.8 ppm) and to the seven protons of the propoxy group H-a, H-b and H-c (δ_H values ranging from 1.1 to 4.2 ppm).

The ^{1}H NMR spectra of **Tx 4**, **Tx 7** and **Tx 11** exhibited characteristic signals for the different protons of the aminated chain; however, the signal corresponding to the NH of the amine could not be observed.

The signals corresponding to the aromatic protons of the amino-halogenated chains of **Tx 4** and **Tx 11** (**Table 7**) appeared from δ_H of 6.9 to 8.4 ppm. Besides, the methylene group of **Tx 4** appear at δ_H 4.34 (d, -CH_2-) ppm.

Table 7 - ^{1}H NMR data* for **Tx 4** and **Tx 11**.

	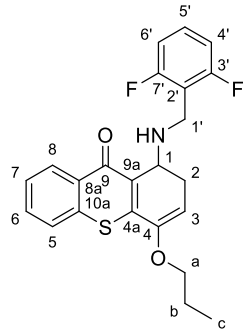 **Tx 4**		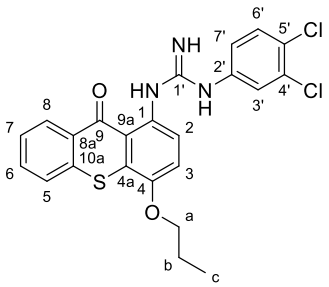 **Tx 11**
	δ_H		**δ_H**
H-8	8.50, 1H, dt, *J* = 8.2 and 1.0	**H-8**	8.76, 1H, dd, *J* = 8.1 and 1.0
H-6	7.52, 2H, m	**H-3'**	8.39, 1H, d, *J* = 2.5
H-5		**H-6**	7.88, 1H, dd, *J* = 8.9 and 2.5
H-7	7.39, 1H, ddd, *J* = 8.2, 4.7 and 3.6	**H-6'**	7.76, 1H, d, *J* = 2.5
H-5'	7.22, 1H, m	**H-2**	7.69, 1H, d, *J* = 9.1
H-4'	6.91, 2H, t, *J* = 7.9	**H-7'**	7.59, 3H, m
H-6'		**H-5**	
H-3	7.15, 1H, d, *J* = 9.1	**H-7**	
H-2	6.75, 1H, d, *J* = 9.1	**H-3**	7.44, 1H, d, *J* = 9.1
H-1'	4.54, 2H, d, *J* = 5.5	**H-a**	4.17, 2H, t, *J* = 6.4
H-a	4.01, 2H, t, *J* = 6.5	**H-b**	1.80, 2H, st, *J* = 7.3
H-b	1.87, 2H, st, *J* = 7.4	**H-c**	1.06, 3H, t, *J* = 7.3
H-c	1.11, 3H, t, *J* = 7.4		

*Values in ppm (δ_H) relative to $(CH_3)_4Si$ as an internal reference. *J* values are in Hz.

The spectrum of **Tx 7** (**Table 8**) also revealed the presence of the signals that correspond to the three aromatic protons of the amino-halogenated chain (δ_H 7.5–7.0 ppm). Moreover, the presence of a quintet at δ_H 2.2 ppm (H-3') coupled with two quartets at δ_H 4.1 pmm (H-4') and δ_H 3.8 ppm (H-2') revealed the presence of the six protons of the methylene groups of the aminated side chain.

Table 8 - ^{1}H NMR data* for **Tx 7**.

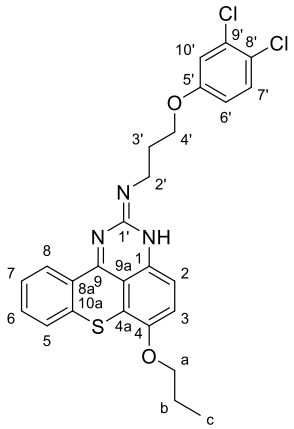

Tx 7

	δ_H		δ_H
H-8	8.77, 1H, dd, *J* = 8.0 and 1.3	**H-6'**	6.74, 1H, dd, *J* = 8.9 and 2.9
H-6	7.46, 2H, m	**H-a**	4.11, 4H, td, *J* = 6.2 and 4.8
H-7'		**H-4'**	
H-5	7.34, 4H, m	**H-2'**	3.78, 2H, q, *J* = 6.2
H-7		**H-3'**	2.19, 2H, p, *J* = 6.2
H-2		**H-b**	1.91, 2H, st, *J* = 7.2
H-3		**H-c**	1.12, 3H, t, *J* = 7.2
H-10'	6.99, 1H, d, *J* = 2.9		

*Values in ppm (δ_H) relative to $(CH_3)_4Si$ as an internal reference. *J* values are in Hz.

1.3.3. ^{13}C NMR data

The data corresponding to the ^{13}C NMR of synthesized compounds **Tx 2**, **4**, **5**, and **7** are represented in **Tables 9–12**.

1.3.3.1. ^{13}C NMR for aminated derivatives Tx 2 and Tx 5

The ^{13}C NMR data of compounds **Tx 2** and **Tx 5** (**Table 9**) showed the presence of two signals with the high chemical shift value corresponding to the carbon of guanidinium group ($\delta_{C\text{-}1'}$: 159.8–159.9 ppm) followed by the carbon of imine group ($\delta_{C\text{-}9}$: 157.9–159.2 ppm). The absence of signal corresponding to the carbonyl group and the appearance of the signal corresponding to the guanidinium group was evidenced on ^{13}C NMR spectrum of both thiochromene quinazolines. This evidence confirmed the intramolecular dehydrative cyclization.

Table 9 - ^{13}C NMR data* for **Tx 2** and **Tx 5**.

	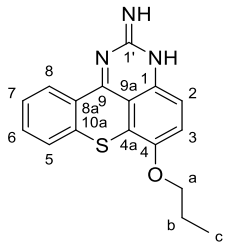 **Tx 2**	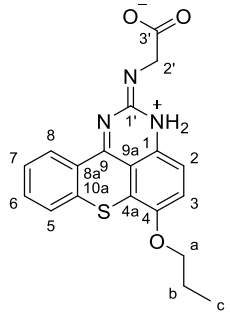 **Tx 5**
	δ_C	**δ_C**
C-1	149.29	148.14
C-2	120.01	119.59
C-3	120.60	119.87
C-4	145.21	146.64
C-4a	117.37	119.65
C-5	127.01	126.90
C-6	131.86	131.62
C-7	126.57	126.35
C-8	127.01	127.90
C-8a	126.85	126.55
C-9	157.89	159.18
C-9a	113.52	115.16
C-10a	134.94	136.34
C-a	70.91	71.56
C-b	22.31	22.83
C-c	10.54	10.65
C-1'	159.84	159.94
C-2'	———	29.71
C-3'	———	207.10

*Values in ppm (δ_C) relative to $(CH_3)_4Si$ as an internal reference.

Moreover, signals corresponding to the carbons linked to the amine group ($\delta_{C\text{-}1}$: 148.2–149.3 ppm) and ether chain ($\delta_{C\text{-}4}$: 145.2–145.6 ppm) are also present. The lowest values shifts ($\delta_{C\text{-}a\text{-}C\text{-}c}$: 10.5–71.6 ppm) correspond to the three carbons of the propoxy groups. The signals corresponding to the remaining ten carbons of the thioxanthone scaffold presented values ranging from 113.5 to 136.3 ppm.

The signal appearing at δ_C 207.1 ppm and δ_C 29.7 ppm corresponded to the carbonyl group of the carboxylic acid and to the methylene group ($-CH_2-$) of the amine moiety of **Tx 5**, respectively.

The carbon assignments were also accomplished by HSQC and HMBC experiments. The HMBC data were important to deduce the chemical shifts of the quaternary carbons and confirm the C-N coupling product. The main connectivities found from HMBC for **Tx 2** and **Tx 5** are depicted in **Figure 17**.

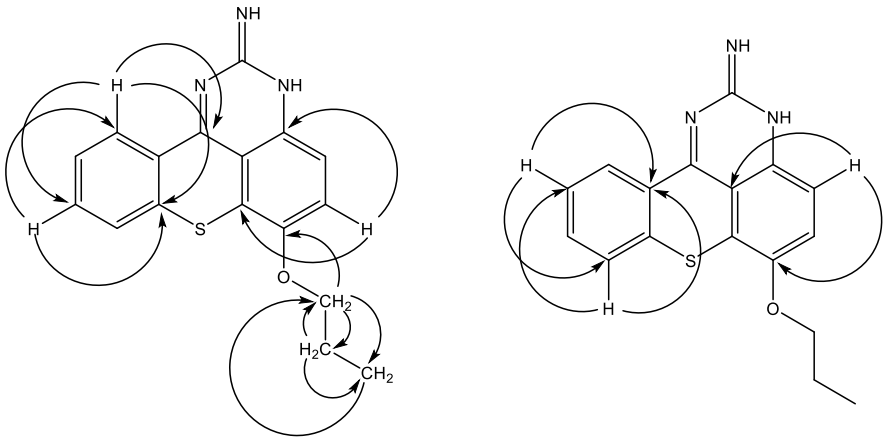

Tx 2

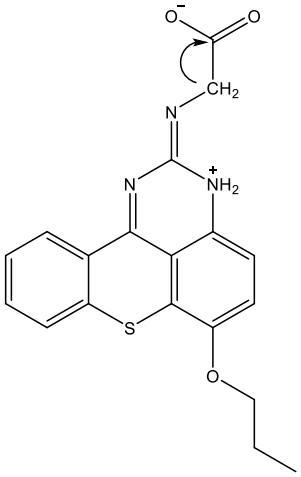

Tx 5

Figure 17 - Main correlations between carbons and protons in HMBC spectrum of **Tx 2** and **Tx 5**.

1.3.3.2. ^{13}C NMR for TxBr

The ^{13}C NMR spectrum of **TxBr** revealed the presence of one signal with the highest chemical shift value corresponding to the carbon of carbonyl group (δ_{C-9}: 180.5 ppm). Moreover, the signal corresponding to the carbon linked to the ether chain (δ_{C-4}: 153.3 ppm) is also present. The lowest values shifts ($\delta_{C-a-C-c}$: 10.8 - 71.4 ppm) correspond to the three carbons of the propoxy group. The signals corresponding to the remaining ten carbons of the thioxanthone scaffold presented values ranging from 113.2 to 135.7 ppm.

The data corresponding to the ^{13}C NMR of **TxBr** is represented in **Table 10**.

Table 10 - ^{13}C NMR data* for **TxBr**.

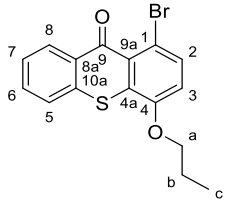

TxBr

	δ_C		δ_C
C-1	113.7	**C-8**	129.8
C-2	133.2	**C-8a**	135.7
C-3	113.2	**C-9**	180.5
C-4	153.3	**C-9a**	127.4
C-4a	130.6	**C-10a**	130.5
C-5	126.1	**C-a**	71.4
C-6	132.1	**C-b**	22.6
C-7	126.7	**C-c**	10.8

*Values in ppm (δ_C) relative to $(CH_3)_4Si$ as an internal reference.

For **TxBr**, ^{13}C NMR assignments of the hydrogenated carbons were determined by HSQC and the carbon atoms not directly bonded to hydrogen atoms were deduced by HMBC experiments. The main connectivities found from HMBC for **TxBr** can be seen in **Figure 18**.

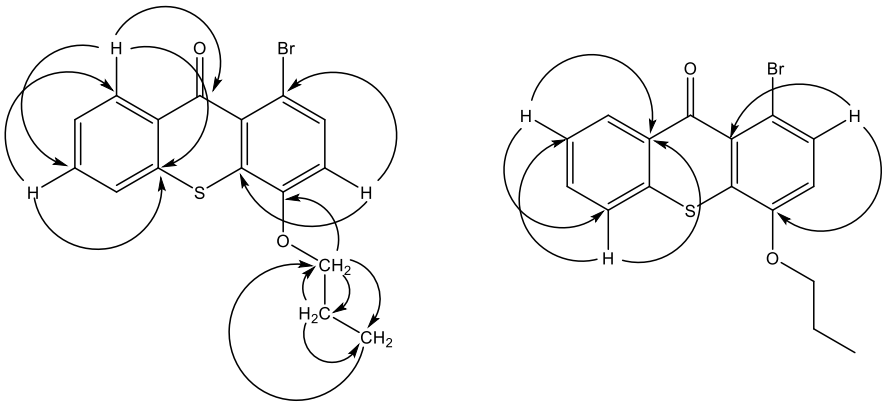

Figure 18 - Correlations between carbons and protons in HMBC spectrum of **TxBr**.

1.3.3.3. ^{13}C NMR for amino-halogenated derivatives Tx 4, Tx 7 and Tx 11

The ^{13}C NMR spectra for compounds **Tx 4** and **Tx 11** (**Table 11**) revealed the presence of signals corresponding to the carbons atoms of the carbonyl group ($\delta_{C\text{-}9}$: 183.4–183.5 ppm), the two aromatic rings (δ_C values ranging from 106 to 148 ppm) and the three carbons of the propoxy group (δ_C values between 10.5 and 72.5 ppm).

Table 11 - ^{13}C NMR data* for **Tx 4** and **Tx 11**.

	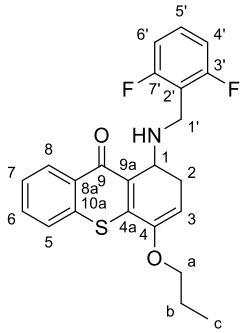 **Tx 4**	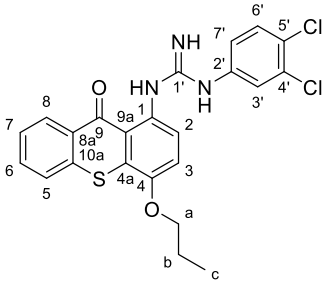 **Tx 11**
	δ_C	**δ_C**
C-1	148.44	143.09
C-2	106.23	116.72
C-3	119.81	121.08
C-4	142.89	146.67
C-4a	130.12	128.62
C-5	125.86	123.95
C-6	131.59	132.22
C-7	125.83	123.07
C-8	129.22	130.30
C-8a	129.35	130.42
C-9	183.41	183.50
C-9a	113.36	119.47
C-10a	136.68	137.17
C-a	72.50	70.82
C-b	22.91	22.28
C-c	10.72	10.53
C-1'	35.04	158.18
C-2'	111.35	141.34
C-3'	161.69	125.75
C-4'	111.65	129.15
C-5'	111.32	122.11
C-6'	111.65	121.24
C-7'	161.69	120.40

*Values in ppm (δ_C) relative to $(CH_3)_4Si$ as an internal reference.

In the aromatic region of these amino-halogenated thioxanthones, the presence of additional signals was evidenced corresponding to the six aromatic carbons of the halogenated aromatic amine precursor and the carbons positioned *ortho* are subjected a higher deshielding effect in relation to *meta* carbons due to the inductive electron withdrawing effect of the halogen atoms. For **Tx 4**, NMR data of this derivative also revealed

an increase of the chemical shift value of the carbons directly linked to halogen atoms with the increase of the electronegativity of the halogen. The signal that appeared at δ_C 35.0 ppm correspond to the carbon of the methylene group (-CH_2-) of the aminated chain. The ^{13}C NMR of compound **Tx 11** also showed the presence of a signal with a high chemical shift value corresponding to the carbon of the guanidinium group ($\delta_{C\text{-}1'}$: 158.2 ppm).

Table 12 - ^{13}C NMR data* for **Tx 7**.

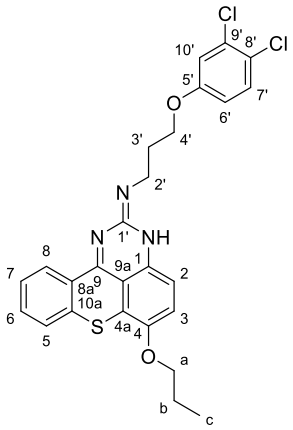

Tx 7

	δc		δc
C-1	135.17	**C-a**	71.61
C-2	119.86	**C-b**	22.86
C-3	119.91	**C-c**	10.66
C-4	146.21	**C-1'**	158.86
C-4a	119.53	**C-2'**	38.59
C-5	126.22	**C-3'**	29.47
C-6	131.42	**C-4'**	66.38
C-7	126.54	**C-5'**	157.97
C-8	127.66	**C-6'**	114.49
C-8a	127.60	**C-7'**	130.59
C-9	158.29	**C-8'**	123.82
C-9a	114.93	**C-9'**	132.77
C-10a	136.28	**C-10'**	116.34

*Values in ppm (δ_C) relative to $(CH_3)_4Si$ as an internal reference.

The ^{13}C NMR data of compound **Tx 7** (**Table 12**) showed the presence of a signal with the highest chemical shift value corresponding to the carbon of guanidinium group ($\delta_{C\text{-}1'}$: 158.9 ppm). The absence of signal corresponding to the carbonyl group (C=O) and the appearance of the signal corresponding to the guanidinium group confirmed the intramolecular dehydrative cyclization. Moreover, signals corresponding to the carbons of the two aromatic rings (δ_C 114.9–136.3 ppm) and ether chains ($\delta_{C\text{-}5'}$: 158.0 ppm and $\delta_{C\text{-}4}$: 146.2 ppm) are also present. In the aromatic region of this derivative, it was evidenced the

presence of additional signals corresponding to the aromatic carbons of the amine precursor (δ_C 114.5–132.8 ppm). The lowest values shifts (δ_C: 10.7–71.6 ppm) correspond to the carbons of the propoxy group and to non-aromatic carbons of the halogenated aromatic amine chain.

The derivatives **Tx 4**, **Tx 7** and **Tx 11** were structurally elucidated by HQSC to identify the chemical shifts of hydrogenated carbons and by HMBC to deduce the chemical shifts of carbon atoms not directly bonded to hydrogen atoms. The main connectivities found from the HMBC for these derivatives can be seen in **Figure 19**.

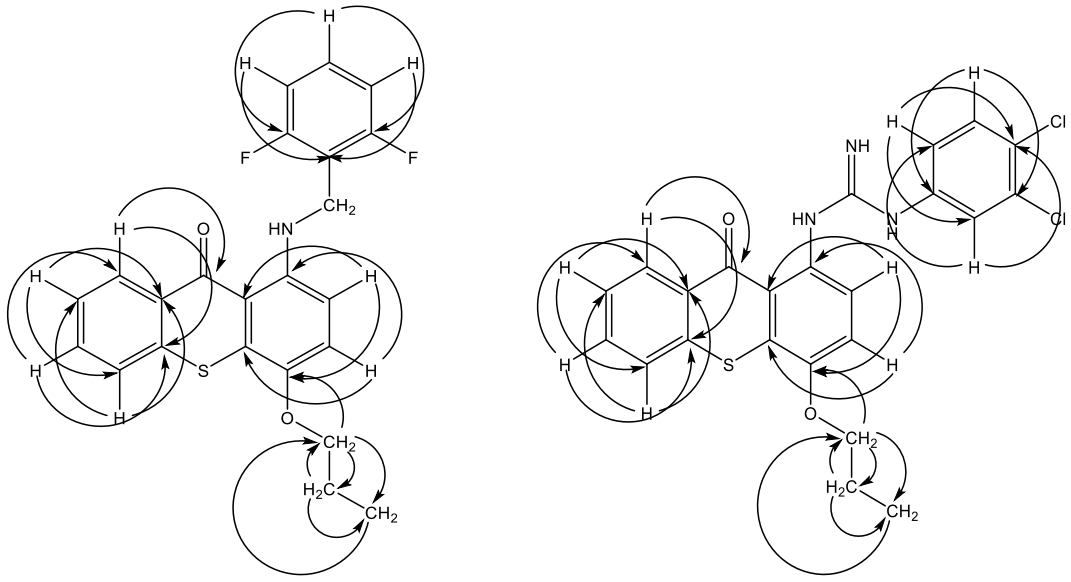

Tx 4

Tx 11

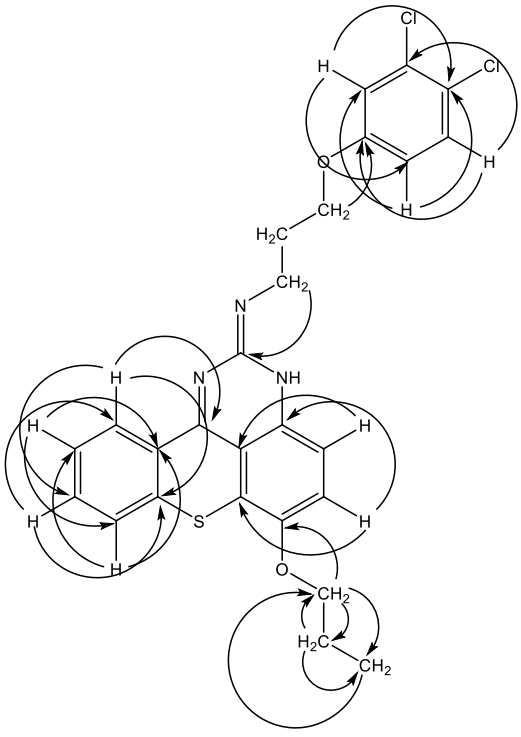

Tx 7

Figure 19 - Correlations between carbons and protons in HMBC spectrum of **Tx4**, **Tx 7** and **Tx 11**.

PART 2 – Antifungal Activity

2.1. Antifungal activities

Prior to investigating the effect of combining the synthetized compounds **Tx 2**, **Tx 4**, **Tx 5**, and **Tx 7** with two azoles, fluconazole (FLC) and voriconazole (VOR), the MIC values of these compounds were determined individually against two different reference *Candida* strains and one clinical resistant *Candida* strain. Also, the methoxylated derivative **TxOMe** (**Figure 14**) and two others amino-thioxanthonic derivatives **TxA1** and **Tx53** (**Figure 12**), previously synthesized in our research group[18] also were evaluated for antifungal activity since they were previously found as inhibitors of a mammalian efflux pump, P-gp.

Three different *Candida* strains were used in the study. The MICs of FLC and VOR, based on an 50% reduction in growth were determined for each *Candida* spp. tested (**Table 13**). According to CLSI guidelines, since the endpoints for azoles are typically less defined, endpoints are read as the lowest drug concentration that produce an approximately 50% reduction in growth. Interpretive breakpoints for *in vitro* susceptibility testing of *Candida* spp. to FLC are: susceptible ≤ 8 µg/mL; susceptible–dose-dependent 16–32 µg/mL and resistant ≥ 64µg/mL; are to VOR are susceptible ≤ 1 µg/mL; susceptible–dose-dependent 2 µg/mL and resistant ≥ 4µg/mL.

For azole-susceptible *C. albicans* (control strain ATCC 10231) the MIC_{50} values for FLC and VOR were 2 and 0.25 µg/mL, respectively; and for *C. krusei* (control strain ATCC 6258), that exhibit intrinsic FLC resistance, the MIC_{50} values were 32 and 0.5 µg/mL, respectively, which are within the reference ranges. For azole-resistant *C. albicans* (clinical strain H37[77]) for FLC the MIC_{50} was >128 µg/mL and for VOR the was >16 µg/mL. The results are presented in **Table 13**.

Table 13 - *Candida* strains used and their susceptibility to azoles.

Strain	MIC_{50} (categorization according breakpoints by CLSI)[71]	
	Fluconazole	**Voriconazole**
C. albicans H37	>128 µg/mL (Resistant)	>16 µg/mL (Resistant)
C. albicans ATCC 10231	2 µg/mL (Susceptible)	0.25 µg/mL (Susceptible)
C. krusei ATCC 6258	32 µg/mL (Resistant)	0.5 µg/mL (Susceptible)

The MIC_{50} values were determined as the lowest concentration of the compound revealed at least 50% growth inhibition.

Based on complete inhibition (MIC_{100}), none of the synthetized compounds revealed antifungal activity against the tested strains. Only one of the seven tested compounds exhibited antifungal activity against the different *Candida* species and strains. The amino-thioxanthone derivative **TxA1** was active against the three tested *Candida* strains with MIC values comprised between 8 and 32 µg/mL (**Table 14**).

Taking in account trailing phenomenon, observed during the tests of *C. albicans* susceptibility to azoles, that difficult the reading results, for the study of the synergistic activity the MIC values of azoles against yeast strains tested were determined based on 100% growth inhibition.

Table 14 - Antifungal activity of thioxanthones. MICs* are expressed in µg/mL.

Compound	*C. albicans* H37	*C. albicans* ATCC 10231	*C. krusei* ATCC 6258
Tx 2	>64	>64	>64
Tx 4	>64	>64	>64
Tx 5	>64	>64	>64
Tx 7	>64	>64	>64
TxOMe	>64	>64	>64
TxA1	32	16	8
Tx53	>64	———	———
FLC	>128	>128	>128
VOR	>16	>16	>16

*The MIC values were determined as the lowest concentration of the compound revealed 100% growth inhibition. Quality control was performed by testing the inhibitory activity of fluconazole with the reference *C. krusei* ATCC 6258.

Despite thioxanthonic derivatives do not exhibited antifungal activity against the tested yeasts, the synergism effect between these compounds and two azole antifungal drugs were evaluated. However, *in vitro* susceptibility assays are highly dependent on the fungal species under investigation, and other method-specific factors. Thus, firstly was tested a yeast model that reverses the antifungal resistance. Based on studies of the synergistic effect between amiodarone and azoles in *Candida* strains[78-79], the three yeasts were tested.

2.2. Synergistic activity of azoles with amiodarone

In order to evaluate the synergistic effect of thioxantonic derivatives (**Tx 2**, **Tx 4**, **Tx 5**, **Tx 7**, **TxOMe**, **TxA1** and **Tx53**) with azoles (FLC and VOR) against the *Candida* strains, firstly was evaluated the capacity of the three yeast strains revert azole-resistance by combination whit amiodarone (AMD).

AMD is an antiarrhythmic drug classically used for the treatment of atrial fibrillation[78]. Recently, AMD was reported to have fungicidal activity against several species, including a variety of clinically important fungi, such as *C. albicans*, *C. neoformans*, *Fusarium oxysporum*, and *Aspergillus nidulans*[80-81]. Researchers also showed that the combination of low doses of AMD with azoles *in vitro* exhibited a synergistic effect against strains of *C. albicans*, *C. neoformans*, and *A. fumigatus*[79, 82-84].

To evaluate the potential synergistic effect between azoles (FLC and VOR) and AMD in three *Candida* spp., a microdilution checkerboard assay according to CLSI M27-A3[71] was performed.

AMD activity varies depending on the pH[85]. Thus, the working pH was established in order to obtain the biggest AMD effect. MIC values for AMD against *Candida* spp. tested showed significant variation as a function of pH, wherein at pH 7 the MIC value was 1000 µM for all yeast tested and at pH 5 the MIC value was much lower (MIC 25 µM). Conversely, the FLC and VOR MICs obtained at pH 5 showed no significant differences compared to those obtained at pH 7. These observations were consistent with previously reported studies[79]. Thus, RPMI 1640 medium at pH 5 was adopted for the experiments with AMD and the two azoles.

Firstly, the MIC values of each drug were determinate, then the cells were exposed to various concentrations of FLC (or VOR) in combination with 10 µM AMD (sub-inhibitory concentration). The interaction between azoles (FLC and VOR) and AMD were determined by calculating the fractional inhibitory concentration (FIC) index (FICI). The FICI was calculated as the sum of the FICs of either drug: FICI = FIC of AMD + FIC of azole = (MIC of AMD in combination with azole/MIC of AMD alone) + (MIC of azole in combination with AMD/MIC of azole alone). The FICI ≤ 0.5 represents synergy, an FICI > 4 antagonism, and a 0.5 < FICI ≤ 4 no interaction[77].

The results of the synergistic effect of azoles and AMD are represented in **Table 15**.

Table 15 - Synergistic effect of azoles and amiodarone (AMD) against *Candida* strains[a].

Drug and strain	MIC_{100}[b]				FLC-AMD interaction	
	Alone		Combination			
	Azole	AMD	Azole	AMD	FICI	IN[c]
Fluconazole						
C. albicans H37	>512	25	0.06	10	0.400	SYN
C. albicans ATCC 10231	>128	25	1	10	0.408	SYN
C. krusei ATCC 6258	32	25	16	10	0.900	NI
Voriconazole						
C. albicans H37	>64	25	≤0.008	10	0.400	SYN
C. albicans ATCC 10231	>16	25	0.03	10	0.402	SYN
C. krusei ATCC 6258	0.25	25	0.03	10	0.520	NI

[a]MICs and FICI values were obtained for all strains according to CLSI document M27-A3 using RPMI 1640 medium buffered at pH 5.
[b]MIC values are expressed in µg/mL for FLC and in µM for AMD. "Combination" refers to the MIC of each drug in combination with the other. These MIC combinations together with the standard MICs were used to obtain the FICI values displayed in the table.
[c]IN, interpretation;.SYN, synergism; NI, no interaction.

Based on complete inhibition (MIC_{100}), all strains showed the same AMD MIC (25 µM), whereas the azole MICs ranged from 32 to >512 µg/ml for FLC and 0.25 to >64 for VOR. When combined with FLC or VOR, AMD in sub-inhibitory concentration of 10 µM showed strong synergistic inhibitory effects against the clinical isolate *C. albicans* H37 with FICI values of 0.40, demonstrating that AMD increased the susceptibility of resistant *C. albicans* to azoles.

Despite *C. albicans* ATCC 10231 being considered a susceptible strain, with MIC_{50} of 2 µg/mL, due to the long trailing growth effect by higher azole concentrations, we did observe higher MIC_{100} values for this strain. AMD when combined with the FLUC and VOR, showed a strong reduction of the MIC values in the *C. albicans* ATCC 10231 by inhibiting the trailing growth.

On the other hand, for the non-*albicans Candida* with intrinsic resistance (*C. krusei* ATCC 6258), the MIC of FLC or VOR showed almost no change when combined with AMD with FICI ranging from 0.52 to 0.90, indicating no interaction between amiodarone and azoles (FLC and VOR).

Since, AMD reversed *C. albicans* H37 resistance phenotype, this yeast model was used to test the thioxanthonic derivative compounds.

2.3. Synergistic activity between azoles and thioxantones

Having established the individual MIC values for **Tx 2**, **Tx 4**, **Tx 5**, **Tx 7**, **TxOMe**, **TxA1**, **Tx53**, FLC, and VOR, the MIC values of thioxanthonic derivatives in combination

with the two azoles (FLC and VOR) were determined in checkerboard assays against the three *Candida* spp., using the CLSI standard reference method (M27-A3) for broth dilution antifungal susceptibility testing of yeasts[71]. When combined with FLC, none compound showed synergistic inhibitory effects against the *Candida* strains tested (**Table 16**).

Table 16 - Susceptibility of yeast strains to thioxanthones (**Tx**) and FLC alone and in combination.

Tx and strain	MIC_{100} (µg/mL)				Interpretation
	Alone		Combination		
	FLC	Tx	FLC	Tx	
Tx 2					
C. albicans H37	>128	>64	>128	>64	NI
C. albicans ATCC 10231	>128	>64	>128	>64	NI
C. krusei ATCC 6258	>128	>64	>128	>64	NI
Tx 4					
C. albicans H37	>128	>64	>128	>64	NI
C. albicans ATCC 10231	>128	>64	>128	>64	NI
C. krusei ATCC 6258	>128	>64	>128	>64	NI
Tx 5					
C. albicans H37	>128	>64	>128	>64	NI
C. albicans ATCC 10231	>128	>64	>128	>64	NI
C. krusei ATCC 6258	>128	>64	>128	>64	NI
Tx 7					
C. albicans H37	>128	>64	>128	>64	NI
C. albicans ATCC 10231	>128	>64	>128	>64	NI
C. krusei ATCC 6258	>128	>64	>128	>64	NI
TxOMe					
C. albicans H37	>128	>64	>128	>64	NI
C. albicans ATCC 10231	>128	>64	>128	>64	NI
C. krusei ATCC 6258	>128	>64	>128	>64	NI
TxA1					
C. albicans H37	>128	32	0.25	32	NI
C. albicans ATCC 10231	>128	16	0.25	16	NI
C. Krusei ATCC 6258	>128	8	0.25	8	NI
Tx53					
C. albicans H37	>128	>64	>128	>64	NI

MICs and FICI values were obtained for all strains according to CLSI document M27-A3 using RPMI 1640 medium buffered at pH 7. NI, no interaction.

Likewise, no synergistic effects were observed by combination of VOR with thioxanthone derivatives against all *Candida* strains tested (**Table 17**).

Table 17 - Susceptibility of yeast strains to thioxanthones (**Tx**) and VOR alone and in combination.

Tx and strain	MIC_{100} (µg/mL)				Interpretation
	Alone		Combination		
	VOR	Tx	VOR	Tx	
Tx 2					
C. albicans H37	>16	>64	>16	>64	NI
C. albicans ATCC 10231	>16	>64	>16	>64	NI
C. krusei ATCC 6258	>16	>64	>16	>64	NI
Tx 4					
C. albicans H37	>16	>64	>16	>64	NI
C. albicans ATCC 10231	>16	>64	>16	>64	NI
C. krusei ATCC 6258	>16	>64	>16	>64	NI
Tx 5					
C. albicans H37	>16	>64	>16	>64	NI
C. albicans ATCC 10231	>16	>64	>16	>64	NI
C. krusei ATCC 6258	>16	>64	>16	>64	NI
Tx 7					
C. albicans H37	>16	>64	>16	>64	NI
C. albicans ATCC 10231	>16	>64	>16	>64	NI
C. krusei ATCC 6258	>16	>64	>16	>64	NI
TxOMe					
C. albicans H37	>16	>64	>16	>64	NI
C. albicans ATCC 10231	>16	>64	>16	>64	NI
C. krusei ATCC 6258	>16	>64	>16	>64	NI
TxA1					
C. albicans H37	>16	32	0.125	32	NI
C. albicans ATCC 10231	>16	16	0.125	16	NI
C. krusei ATCC 6258	>16	8	0.125	8	NI
Tx53					
C. albicans H37	>16	>64	>16	>64	NI

MICs and FICI values were obtained for all strains according to CLSI document M27-A3 using RPMI 1640 medium buffered at pH 7. NI, no interaction.

Opportunistic fungal infections have become a serious threat to human health due to the rising population of patients with low immunity as result of HIV infections, chemotherapy, and organ transplant[86].

Between these fungi, *C. albicans* is the most frequently observed opportunistic human pathogen causing mucosal and systemic infections in immunocompromised individuals[87]. However, a notable increase in infections caused by non-*albicans Candida* species has been reported [88].

In virtue of great efficacy and low toxicity, azoles have been extensively used in clinical practice to treat various fungal infections in humans, including candidiasis. However, as the use of azole antifungal agents has risen dramatically, there has been an increase in the number of reports of azole-resistant isolates of *Candida*[88]. Thus, new strategies are warranted to overcome antifungal drug resistance. Combination therapies of antifungal drugs with non-antifungal agents might be an ideal approach to treat candidiasis caused by drug-resistant *Candida* spp.

Studies have reported the *in vitro* synergistic effect of AMD with azoles against azole-resistant strains of *C. albicans* and *A. fumigatus*[79, 82, 84]. Knorre *et al*. (2009) have reported that the treatment of azole-resistant strains of *S. cerevisiae* with AMD decreased MDR due to the inhibition of cellular efflux pumps[89]. Here, we found that the combination of AMD with FLC and VOR, showed a synergism against the resistant *C. albicans in vitro*. The MICs of the azoles against resistant *C. albicans* H37 decreased from > 512 μg/mL to 0.06 μg/mL for FLC, and from > 64 μg/mL to ≤ 0.008 μg/mL to VOR in presence of AMD.

The mechanism of *in vitro* resistance to azole antifungal drugs in the human pathogen *C. albicans* H37 is the inactivation of *ERG3*, a gene encoding sterol $\Delta^{5,6}$-desaturase, a key enzyme in ergosterol biosynthesis, consequently does not have sterol (replaced by the accumulation of ergosta-7,22-dienol). Since *C. albicans* H37 use a different sterol, it is possible that this contributes for alterations in plasmatic membrane, including alterations in efflux pumps[77].

AMD is a therapeutic agent used in the treatment of life-threatening ventricular arrhythmias and supraventricular dysrhythmias, that have been demonstrate fungicidal activity[83]. Several studies have been carried out in order to identify the mechanism of AMD-azole synergy. Guo *et al*. (2008) proposed that since, in cardiac cells, AMD inhibits L-type Ca^{2+} channels and Na^{+}/K^{+} channels; the mechanism of the synergistic effect between AMD and azoles was a consequence of disrupted Ca^{2+} homeostasis[84]. According to Gamarra *et al*. (2010), the synergism activity of the FLC-AMD combination in FLC-resistant *C. albicans* strains can be explained by efflux pump blockage caused by AMD[79]. Other possible mechanisms were also described, including changes in the integrity of the yeast cell membrane and the generation of oxidative stress, mitochondrial dysfunction, and DNA damage that could lead to cell death by apoptosis[78].

Moreover, the data reported here show that AMD was able to enhance the activity of two azoles (FLC and VOR) against the *C. albicans* ATCC 10231 that display the trailing growth phenomenon. However, no interaction was observed when AMD was used combined with azoles against *C. krusei*.

Mai *et al*. (2007) reported two chloro-containing uracil-hydroxamates that were able to reduce the MIC values of FLC on *Candida* strains that show the trailing effect. However, the molecular mechanism of action has not yet been established[90].

It is well known that a decrease in the drug concentration in the fungal cells could be induced by the over-expression of efflux pumps[91]. Numerous studies suggest that inhibiting the function of the efflux pump might be an important synergistic mechanism of drug interactions against resistant isolates[92-93].

Thioxanthones are an important class of molecules showing interesting biological properties, namely efflux pump inhibition[1]. Several studies have been demonstrating the thioxanthones ability of modulate the human efflux pump P-gp[18, 94], although the studies on their ability to inhibit microbial efflux pump activity are still sparse[13].

In order to find inhibitors of fungal efflux pumps and, thereby overcoming antifungal drug resistance, the yeasts were exposed to different thioxanthonic derivatives in combination with two azoles, FLC and VOR. In this study, we investigated the *in vitro* antifungal synergy of seven amino-thioxanthonic derivatives, **Tx 2**, **Tx 4**, **Tx 5**, **Tx 7**, **TxOMe**, **TxA1**, and **Tx53**, with two azoles (FLC and VOR) against the three *Candida* spp. Our results demonstrated that none of the compounds exhibit antifungal synergy *in vitr*o with both azoles against the *Candida* strains tested.

Nevertheless, further studies on bacterial models with the efflux transporters overexpressed must be performed to ascribe the potential of these new derivatives as EPIs and adjuvants in the antimicrobial arsenal.

CHAPTER IV:
CONCLUSIONS

IV. Conclusions

The identification of efflux pumps inhibitors constitutes a valuable strategy to revert antifungal drug resistance. Since that thioxanthonic derivatives and, particularly, aminated thioxanthones, have showed inhibitory activity against the human efflux pump P-gp, the potential synergistic combination effects of several thioxanthonic derivatives with azoles against *Candida* species were studied.

Therefore, in order to accomplish the main aim of this study, five amino thioxanthonic derivatives were synthesized by copper-catalyzed nucleophilic aromatic substitution of a suitable functionalized thioxanthone (**TxCl** or **TxBr**) with an appropriated amine. The reaction conditions used for the nucleophilic aromatic substitution of the chlorinated thioxanthone **TxCl** allowed a successful synthesis of the brominated thioxanthone **TxBr**. The reaction conditions used Ullmann cross coupling reaction allowed the synthesis of two 1-amino-halogenated 4-propoxy-9*H*-thioxanthen-9-ones (**Tx 4** and **Tx 11**) and three unexpected thiochromeno[4,3,2-*de*]quinazolines (**Tx 2**, **Tx 5** and **Tx 7**). However, the obtained yields were very low. These results were not expected, since this methodology had been applied in this research group for the synthesis of other aminated thioxanthones with higher yields.

Spectroscopic methods (IR, ^{1}H NMR, ^{13}C NMR, and bidimensional HSQC and HMBC) allowed the elucidation of all the thioxanthonic derivatives. Moreover, the purification process applied allowed to obtain the desirable thioxanthones with a purity of at least 95 % and with enough amounts to proceed with the evaluation of their biological activity.

The assay carried out for evaluation of the synergistic activity between the azole antifungal drugs and thioxanthones (**Tx 2**, **Tx 4**, **Tx 5**, **Tx 7**, **TxOMe**, **TxA1**, **Tx53**) demonstrated that none of the compounds exhibited synergistic interactions. Among all the aminated thioxanthones tested, **TxA1** was the only that demonstrated antifungal activity *in vitro*.

Considering the results obtained in the evaluation of the synergistic effect of azoles with amiodarone, our study proved the synergistic combination effects between AMD and two azoles against the azole-resistant *C. albicans* tested. Moreover, AMD showed a strong reduction of the azoles MIC_{100} values against the *C. albicans* that display the trailing growth phenomenon, by inhibiting this event.

Future work will involve the study of other biological activities, namely studies on bacterial models with the efflux transporters overexpressed.

CHAPTER V:
MATERIAL AND METHODS

V. Material and Methods

PART 1 – CHEMISTRY

1.1. General methods

All the reagents and solvents were purchased from Sigma Aldrich and had no further purification. Solvents were evaporated using rotary evaporator under reduced pressure, Buchi Waterchath B-480.

All reactions were monitored by TLC carried out on precoated plates with 0.2 mm of thickness using Merck silica gel 60 (GF254). The UV light at 254 and 365 nm or/and chemical were used for visualization of chromatograms.

Microwave (MW) reactions were performed in glassware open vessel reactors in a MicroSYNTH 1600 Microwave Labstation from Millestone (ThermoUnicam, Portugal). The internal reaction temperature was controlled by a fiber-optic probe sensor.

Purification of the synthesized compounds was performed by flash column chromatography using Merck silica gel 60 (0.040-0.063 mm), Discovery® DSC-SCX SPE cationic exchange cartridge, and preparative thin layer chromatography (PTLC) using silica gel 60 GF_{254}.

Melting points (mp) were measured in a Köfler microscope and are uncorrected. Infrared (IR) spectra were obtained in KBr microplates in a Fourier transform infrared spectroscopy spectrometer Nicolet iS10 from Thermo Scientific with Smart OMNI-Transmisson accessory (Software OMNIC 8.3) (cm^{-1}).

NMR spectra were performed in University of Aveiro, Department of Chemistry, and were taken in $CDCl_3$ (Deutero GmbH) at room temperature or DMSO-d_6 (Deutero GmbH) at room temperature, on Bruker Avance 300 spectrometer (300.13 MHz for ^{1}H and 75.47 MHz for ^{13}C). ^{13}C NMR assignments were made by bidimentional HSQC and HMBC experiments.

1.2. Synthesis of thioxanthone derivatives

1.2.1. General procedure for the synthesis of 1-aminated 4-propoxy-9*H*-thioxanthen-9-ones

1-Chloro-4-propoxy-9*H*-thioxanthen-9-one (**TxCl**, 250 mg, 0.8 mmol) and the appropriated amine (**A 2** and **A 5**; 1.6 mmol) were dissolved in methanol (25 mL) and CuI (0.15 mmol) and K_2CO_3 (1.6 mmol) were added. The reaction mixture was heated at 100 ºC in a muffle for 48 hours, and monitored by TLC using the mobile phase chloroform/acetone, 9:1 (v/v).

1.2.1.1. 6-Propoxythiochromeno[4,3,2-*de*]quinazolin-2(3*H*)-imine (Tx 2)

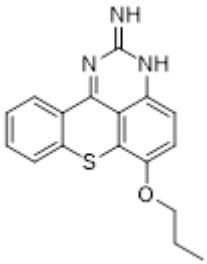

Compound **Tx 2** was synthesized following the protocol described on section 1.2.1. After completing the reaction, the crude material was filtrated, washed with dichloromethane and was concentrated under reduced pressure. Then, a liquid-liquid extraction under acidic and basic solutions was performed. Initially, the crude material was dissolved in 50 mL of chloroform and extracted with HCl 1M (3 × 50 mL). The resulting aqueous layer was basified with NaOH 20% and extracted with chloroform (3 × 100 mL). The organic layers were gathered, dried over anhydrous sodium sulphate and concentrated under reduced pressure. A flash column chromatography (silica gel, dichloromethane/acetone in gradient) was performed in work-up of the crude material. The fractions with the thioxanthone derivative **Tx 2** were gathered and concentrated under reduced pressure. The solid thus obtained was purified by solid phase extraction with a cation exchange cartridge Discovery® DSC-SCX, following the steps: activation of the cartridge with dichloromethane (50 mL); loading the cartridge with the sample (previously incorporated in silica); elution with dichloromethane; elution with a mixture of dichloromethane/acetone 9:1; elution with NH_3 2% in dichloromethane/acetone 9:1. The fractions containing the thioxanthonic derivative were gathered and concentrated under reduced pressure to furnish an orange solid of 6-propoxythiochromeno[4,3,2-*de*]quinazolin-2(3*H*)-imine (**Tx 2**, 44.5 mg, 17.58%).

6-Propoxythiochromeno[4,3,2-*de*]quinazolin-2(3*H*)-imine (**Tx 2**): m.p. 222-224 ºC; IR (KBr) υ_{max} (cm^{-1}): 3297, 3157, 2963, 1640, 1569, 1558, 1453, 1318, 1261, 1231, 1064, 980, 823, 800, 765, 643, 539, 475; ^{1}H NMR ($CDCl_3$, 300.12 MHz) δ: 8.71 (1H, dd, *J* = 8.2 and 0.9 Hz, H-8), 7.60 (3H, m, H-6, H-5, H-3), 4.46 (1H, ddd, *J* = 8.2, 6.6 and 1.7 Hz, H-7), 7.22 (1H, d, *J* = 9.1 Hz, H-2), 6.65 (2H, brs, NH), 4.13 (2H, t, *J* = 6.4 Hz, H-a), 1.78 (2H, d, *J* = 7.4 Hz, H-b), 1.05 (3H, d, *J* = 7.4 Hz, H-c); ^{13}C NMR ($CDCl_3$, 75.47 MHz) δ: 159.84 (C-1'), 157.89 (C-9), 149.29 (C-1), 145.21 (C-4), 131.86 (C-6), 134.94 (C-10a), 127.01 (C-8, C-5), 126.85 (C-8a), 126.57 (C-7), 120.60 (C-3), 120.01 (C-2), 117.37 (C-4a), 113.52 (C-9a), 70.91 (C-a), 22.31 (C-b), 10.54 (C-c).

1.2.1.2. 2-((6-Propoxythiochromeno[4,3,2-*de*]quinazolin-3-ium-2(3*H*)-ylidene)amino)acetate (Tx 5)

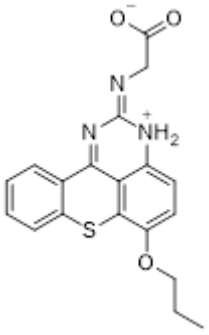

Compound **Tx 5** was synthesized based on the protocol described on section 1.2.1. After completing the reaction, the crude material was filtrated, washed with dichloromethane and was concentrated under reduced pressure. Then, a liquid-liquid extraction under acidic and basic solutions was performed. Initially, the crude material was dissolved in 50 mL of chloroform and extracted with HCl 1M (3 × 50 mL). The resulting aqueous layer was basified with NaOH 20% and extracted with chloroform (3 × 100 mL). The organic layers were gathered, dried over anhydrous sodium sulphate and concentrated under reduced pressure. The organic layers were gathered, dried over anhydrous sodium sulphate and concentrated under reduced pressure. A flash column chromatography (silica gel, dichloromethane/acetone 8:2) was performed in work-up of the crude product. The fractions with the thioxanthonic derivative were gathered and concentrated under reduced pressure. The solid thus obtained was purified by solid phase extraction with a cation exchange cartridge Discovery® DSC-SCX, following the steps: activation of the cartridge with dichloromethane (50 mL); loading the cartridge with the sample (previously incorporated in silica); elution with dichloromethane; elution with a mixture of dichloromethane/acetone 9:1; elution with a mixture of dichloromethane/acetone 8:2; elution with NH_3 2% in dichloromethane/acetone 8:2. The fractions containing the thioxanthonic derivatives were gathered and concentrated under reduced pressure to furnish an orange solid of 2-((6-propoxythiochromeno[4,3,2-*de*]quinazolin-2(3*H*)-ylidene)amino)acetic acid (**Tx 5**, 7.0 mg, 2.31%).

2-((6-Propoxythiochromeno[4,3,2-*de*]quinazolin-2(3*H*)-ylidene)amino)acetic acid (**Tx 5**): m.p.: 218-220 ºC; IR (KBr) υ_{max} (cm^{-1}): 3461, 3297, 3157, 2962, 2919, 2850, 1638, 1608, 1545, 1501, 1453, 1318 1260,1063, 979, 906, 823, 765, 725, 539, 421; ^{1}H NMR ($CDCl_3$, 300.12 MHz) δ: 8.80 (1H, dt, *J* = 8.0 and 1.1 Hz, H-8), 7.42 (5H, m, H-6, H-5, H-7, H-2, H-3), 5.22 (2H, brs, NH), 4.13 (2H, t, *J* = 6.4 Hz, H-a), 2.17 (2H, s, H-2'), 1.91 (2H, st, *J* = 7.4 Hz, H-b), 1.13 (3H, t, *J* = 7.4 Hz, H-c);^{13}C NMR ($CDCl_3$, 75.47 MHz) δ: 207.10 (C-3'), 159.94 (C-1'), 159.18 (159.94), 148.14 (C-1), 146.64 (C-4), 136.34 (C-10a), 131.62 (C-6), 127.90 (C-8), 126.90 (C-6), 126.55 (C-8a), 126.35 (C-7), 119.87 (C-3), 119.65 (C-4a), 119.59 (C-2), 115.16 (C-9a), 71.56 (C-a), 29.71 (C-2'), 22.83 (C-b), 10.65 (C-c).

1.2.2. Synthesis of 1-bromo-4-propoxy-9*H*-thioxanthen-9-one (TxBr)

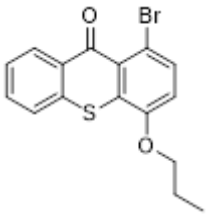

1-Chloro-4-propoxy-9*H*-thioxanthen-9-one (**TxCl**, 1 g, 5 mmol) was treated with KBr (2.98 g, 0.025 mol), CuI (0.028 g, 0.15 mmol), and 85% H_3PO_4 (0.5 mL) in nitrobenzene (8 mL) and the mixture was stirred at reflux for 24 hours. Water was added after cooling to dissolve all inorganic components. The product was extracted with dichloromethane. The dichloromethane was evaporated, and the procedure is repeated one more time, using the mixture as a starting material. After completing the reaction, the crude product was subjected to a flash column chromatography (silica gel, *n*-hexane/ethyl acetate in gradient). The crystallization from the fractions with the thioxanthone in methanol resulted in a pure yellow solid of 1-bromo-4-propoxy-9*H*-thioxanthen-9-one (**TxBr**, 61.8 mg, 53.6%). The experimental procedure described here was adapted from [76].

1-Bromo-4-propoxy-9*H*-thioxanthen-9-one (**TxBr**): m.p. 109-112 ºC; IR (KBr) υ_{max} (cm^{-1}): 2960, 2926, 2874, 1637, 1592,1580, 1549, 1459, 1427, 1306 ,1253 ,1173, 1052, 960, 865, 807, 744, 678, 642, 565, 478; ^{1}H NMR ($CDCl_3$, 300.12 MHz) δ (ppm): 8.45 (1H, dd, *J* = 8.1 and 0.8 Hz, H-8), 7.66 (1H, d, *J* = 8.6 Hz, H-2), 7.58 (2H, m, H-6, H-5), 7.46 (1H, ddd, *J* = 8.1, 5.4, and 2.8 Hz, H-7), 6.89 (1H, d, *J* = 8.6 Hz, H-3), 4.11 (2H, t, *J* = 6.4 Hz, H-a), 1,94 (2H, st, *J* = 7.4 Hz, H-b), 1.16 (3H, t, *J* = 7.4 Hz, H-c); ^{13}C NMR ($CDCl_3$, 75.47 MHz) δ (ppm): 180.5 (C-9), 153.3 (C-4), 135.7 (C-8a), 133.2 (C-2), 132.1 (C-6), 130.6 (C-4a), 130.5 (C-10a), 129.8 (C-8), 127.4 (C-9a), 126.7 (C-7), 126.1 (C-5), 113.7 (C-1), 113.2 (C-3), 71.4 (C-a), 22.6 (C-b), 10.8 (C-c).

1.2.3. General procedure for the synthesis of 1-amino-halogenated 4-propoxy-9*H*-thioxanthen-9-ones

1-Bromo-4-propoxy-9*H*-thioxanthen-9-one (**TxBr**, 1 equiv.) and the amine (**A 4**, **A 7** and **A11**; 2 equiv.) were dissolved in methanol (25 mL) and CuI (0.15 mmol) and K_2CO_3 (1.6 mmol) were added. The reaction mixture was heated at 100 ºC in a muffle for 48 hours, and monitored by TLC using the mobile phase chloroform/acetone, 9:1 (v/v).

1.2.3.1. 1-((2,6-Difluorobenzyl)amino)-4-propoxy-9*H*-thioxanthen-9-one (Tx 4)

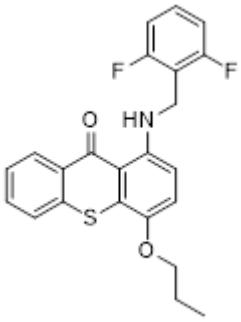

Compound **Tx 4** was synthesized from thioxanthone **TxBr** (250 mg, 7 mmol) and from amine **A 4** (200 mg, 14 mmol), following the protocol described on section 1.2.3. After completing the reaction, the crude material was filtrated, washed with dichloromethane and was concentrated under reduced pressure. Then, the crude material was dissolved in 50 mL of chloroform and extracted with water (3 × 50 mL). The organic layer was dried over anhydrous sodium sulphate and concentrated under reduced pressure. The crude product was purified by a flash column chromatography (silica gel, dichloromethane/petroleum ether 8:2). An orange solid corresponding to 1-((2,6-difluorobenzyl)amino)-4-propoxy-9*H*-thioxanthen-9-one was obtained (**Tx 4**, 6.2 mg, 2.04%).

1-((2,6-Difluorobenzyl)amino)-4-propoxy-9H-thioxanthen-9-one (**Tx 4**): m.p.: 145-147 ºC; IR (KBr) υ_{max} (cm^{-1}): 3270, 2960, 2924, 2849, 1618, 1594, 1560, 1468, 1304, 1274, 1231, 11169, 1050, 957, 784, 748, 421; ^{1}H NMR ($CDCl_3$, 300.12 MHz) δ: 8.50 (1H, dt, *J* = 8.2 and 1.0 Hz, H-8), 7.52 (2H, m, H-6, H-5), 7.39 (1H, ddd, *J* = 8.2, 4.7, and 3.6 Hz, H-7), 7.22 (1H, m, H-5'), 6.91 (2H, t, *J* = 7.9 Hz, H-4', H-6'), 7.15 (1H, d, *J* = 9.1 Hz, H-3), 6.74 (1H, d, *J* = 9.1 Hz, H-2), 4.54 (2H, d, J = 5.5 Hz, H-1'), 4.01 (2H, t, *J* = 6.5 Hz, H-a), 1,87 (2H, st, *J* = 7.4 Hz, H-b), 1.14 (3H, t, *J* = 7.4 Hz, H-c); ^{13}C NMR ($CDCl_3$, 75.47 MHz) δ: 183.4 (C-9), 161.7 (C-3', C-7'), 148.4 (C-1), 142.9 (C-4), 136.68 (C-10a), 131.6 (C-6), 130.1 (C-4a), 125.9 (C-5), 125.8 (C-7), 129.3 (C-8a), 129.2 (C-8), 119.8 (C-3), 106.2 (C-2), 113.4 (C-9a), 111.6 (C-4', C-6'), 111.4 (C-2'), 111.3 (C-5'), 72.50 (C-a), 35.04 (C-1'), 22.91 (C-b), 10.72 (C-c).

1.2.3.2. *N*-(3-(3,4-Dichlorophenoxy)propyl)-6-propoxythiochromeno[4,3,2-*de*]quinazolin-2(3*H*)-imine (Tx 7)

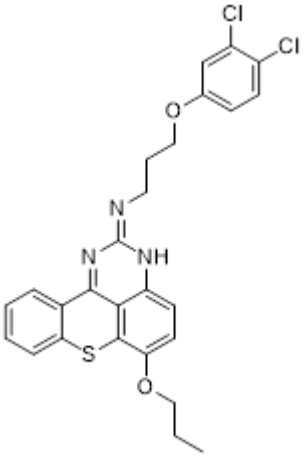

Compound **Tx 7** was synthesized from thioxanthone **TxBr** (100 mg, 3 mmol) and from amine **A 7** (195 mg, 6 mmol), following the protocol described on section 1.2.3. After completing the reaction, the crude material was filtrated, washed with dichloromethane and was concentrated under reduced pressure. Then, the crude material was dissolved in 50 ml of chloroform and extracted with water (3 × 50 mL). The organic layer was dried over anhydrous sodium sulphate and concentrated under reduced pressure. A flash column chromatography (silica gel, chloroform) was performed in work-up of the crude product. The fractions with the thioxanthonic derivative were gathered and concentrated under reduced pressure. The solid thus obtained was purified by preparative thin layer chromatography (PTLC) (silica gel; chloroform/acetone 9:1). to furnish an orange solid of 1-(3-(3,4-dichlorophenoxy)propyl)-3-(9-oxo-4-propoxy-9*H*-thioxanthen-1-yl)guanidine (**Tx 7**, 19.8 mg, 12.24%).

3-(3-(3,4-Dichlorophenoxy)propyl)-6-propoxythiochromeno[4,3,2-*de*]quinazolin-2(3*H*)-imine (**Tx 7**): m.p.: 139-142 ºC; IR (KBr) υ_{max} (cm^{-1}): 3263, 3158, 2924, 2853, 1647, 1556, 1533, 1475, 1382, 1263, 1228, 1123, 1073, 1034, 817, 792, 421; ^{1}H NMR ($CDCl_3$, 300.12 MHz) δ: 8.77 (1H, dt, *J* = 8.0 and 1.3 Hz, H-8), 7.46 (2H, m, H-6, H- 7'), 7.34 (4H, m, H-5, H-7, H-2, H-3), 6.99 (1H, d, *J* = 2.9 Hz, H-10'), 6.74 (1H, dd, *J* = 8.9 and 2.9 Hz, H-6'), 4.11 (4H, dt *J* = 6.2 and 4.8 Hz, H-a, H-4'), 3.78 (2H, q, *J* = 6.2 Hz, H-2'), 2.19 (2H, p, *J* = 6.2 Hz, H-3'), 1.91 (2H, st, J = 7.2 Hz, H-b), 1.12 (3H, t, J = 7.2 Hz, H-c); ^{13}C NMR ($CDCl_3$, 75.47 MHz) δ:158.86 (C-1'), 158.29 (C-9), 157.97 (C-5'), 146.21 (C-4), 136.28 (C-10a), 132.77 (C-9'), 135.17 (C-1), 131.42 (C-6), 130.59 (C-7'), 127.66 (C-8), 127.60 (C-8a), 126.54 (C-7), 126.22 (C-5), 123.82 (C-8'), 119.91 (C-3), 119.86 (C-2),119.53 (C-4a), 116.34 (C-10'), 114.93 (C-9a), 114.49 (C-6'), 71.61 (C-a), 66.38 (C-4'), 38.59 (C-2'), 29.47 (C-3'), 22.86 (C-b), 10.66 (C-c).

1.2.3.3. 1-(3,4-Dichlorophenyl)-3-(9-oxo-4-propoxy-9*H*-thioxanthen-1-yl)guanidine (Tx 11)

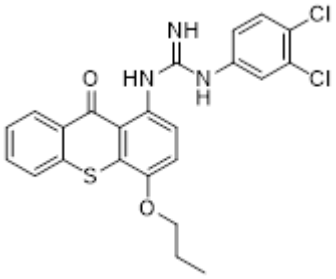

Compound **Tx 11** was synthesized from thioxanthone **TxBr** (47 mg, 0.14 mmol) and from amine **A 11** (125 mg, 2.7 mmol), following the protocol described on section 1.2.3. After completing the reaction, the crude material was filtrated, washed with chloroform and was concentrated under reduced pressure. Then, the crude material was dissolved in 50 ml of chloroform and extracted with water (3 × 50 mL). The organic layer was dried over anhydrous sodium sulphate and concentrated under reduced pressure. A flash column chromatography (silica gel, chloroform) was performed in work-up of the crude product. The fractions with the thioxanthonic derivative were gathered and concentrated under reduced pressure. The solid thus obtained was purified by PTLC (silica gel; chloroform (100%)). Detection and fractioning in PTLC was achieved by UV light (254 nm). Thioxanthone derivative **Tx 11** was washed with chloroform and the solvent was evaporated under reduced pressure to furnish an orange solid 1-(3,4-dichlorophenyl)-3-(9-oxo-4-propoxy-9*H*-thioxanthen-1-yl)guanidine (**Tx 11**, 7.9 mg, 11.15%):

1-(3,4-Dichlorophenyl)-3-(9-oxo-4-propoxy-9*H*-thioxanthen-1-yl)guanidine (**Tx 11**): m.p.: 182-184 ºC; IR (KBr) υ_{max} (cm^{-1}): 3257, 2960, 2922, 2850, 1610, 570, 1553, 1508, 1466, 1263, 1227, 1076, 818, 792, 730, 719, 421; ^{1}H NMR ($CDCl_3$, 300.12 MHz) δ: 8.76 (1H, dd, *J* = 8.1 and 1.0 Hz, H-8), 8.39 (1H, d, *J* = 2.5 Hz, H-3'), 7.88 (1H, dd, *J* = 8.9 and 2.5 Hz, H-6), 7.76 (1H, d, *J* = 2.5 Hz, H-6'), 7.69 (1H, d, *J* = 9.1 Hz, H-2), 7.59 (3H, m, H-7', H-5, H-7), 7.44 (1H, d, *J* = 9.1 Hz, H-3), 4.17 (2H, t, *J* = 6.4 Hz, H-a), 1.80 (2H, st, *J* = 7.3 Hz, H-b), 1.06 (3H, t, *J* = 7.3 Hz, H-c); ^{13}C NMR ($CDCl_3$, 75.47 MHz) δ: 183.50 (C-9), 158.18 (C-1'), 146.67 (C-4),143.09 (C-1), 141.34 (C-2'), 137.17 (C-10a), 132.22 (C-6), 130.42 (C-8a), 130.30 (C-8), 129.15 (C-4'), 128.62 (C-4a), 125.75 (C-3'), 123.95 (C-5), 123.07 (C-7), 122.11 (C-5'), 121.24 (C-6'), 121.08 (C-3), 120.40 (C-7'), 119.47 (C-9a), 116.72 (C-2), 70.82 (C-a), 22.28 (C-b), 10.53 (C-c).

1.3. Determination of thioxanthones purity

The purity of each compound was determined by HPLC-DAD. The HPLC analysis was performed on a Finnigan Surveyor equiped with diode array detector TSP UV8000LP. Chromatographic separation was carried out on 250 × 4.6 mm i.d. FortisBIO C18 column (5 µM) using a mixture of methanol:water (trifluoroacetic acid 0.1%) (80:20 v/v) as mobile phase. The flow rate was set at 1 mL/min. An aliquot of 20 µL of each synthesized thioxanthones (**Tx 2**, **Tx 4**, **Tx 5**, and **Tx 7**) was injected into the HPLC system and the

elution was monitored at 275 nm. The detector was set at a wavelength range of 200– 500 nm with a spectral resolution of 1 nm. The purity parameters included a 95% active peak region and a scan threshold of 5 mAU.

PART 2 – Antifungal Activity

2.1. Strains

The following three *Candida* strains with different susceptibility profiles were used in this study: the azole resistant clinical isolates *C. albicans* H37 (kindly provided by Professor Cidália Pina-Vaz, Faculty of Medicine of the University of Porto, Hospital de S. João, Porto, Portugal), and the American Type Culture Collection (ATCC) reference strains *C. albicans* ATCC 10231 and *C. krusei* ATCC 6258. *C. krusei* ATCC 6258 was also used as a quality control. The strains were stored in Sabouraud dextrose broth (BioMérieux, Marcy L'Etoile, France) with 20% glycerol at −70 ºC. All the strains were subcultured in Sabouraud dextrose agar (SDA; BioMérieux) at 35°C before each experiment to certify optimal growth and purity.

2.2. Drugs

The antifungal agents fluconazole (FLC), voriconazole (VOR) and amiodarone (AMD) were obtained from Sigma-Aldrich (St. Louis, MO, USA). FLC, VOR and AMD were dissolved in DMSO (Sigma-Aldrich, St. Louis, MO, USA) at a concentration of 25.6 mg/mL, 6.4 mg/mL and 10 mM, respectively. The stock solutions of the thioxanthonic derivatives (10 mg/mL) were prepared in DMSO. All these stock solutions were stored at -20 ºC until use.

2.3. Medium

The medium was RPMI 1640 powder medium (with L-glutamine and phenol red, and without $NaHCO_3$; Biochrom®) buffered with 0.165 M MOPS (morpholinepropanesulfonic acid; Sigma-Aldrich, St. Louis, MO, USA). The pH of the medium was adjusted to 7.0 ± 0.1 with NaOH, and to 5.0 ± 0.1 with HCl.

2.4. Antifungal susceptibility testing

The MIC values for each compound were determined by the broth microdilution method according to CLSI guidelines (reference documents M27-A3 for yeasts[71]). Concisely, fungal organism cell suspensions from SDA cultures were prepared in 0.85% NaCl and the transmittance of cell density adjusted to that produced by a 0.5 McFarland standard. To achieve an inoculum size of $1–5\times10^3$ colony forming unit (CFU)/mL, the cell suspensions were diluted with RPMI 1640 medium (pH 7). The stock solutions of the thioxanthonic derivatives (**Tx 2**, **Tx 4**, **Tx 5**, **Tx 7**, **TxA1**, **Tx53** and **TxOMe**) were diluted in serial two-folds with RPMI 1640 medium (pH 7) and added to the cell suspensions in order

to obtain test concentrations ranging from 16 to 64 µg/mL. DMSO was always <1% (v/v) of the total volume of medium. Wells without the drugs that served as the growth control, wells with only RPMI1640 medium (pH 7) that served as the sterility control and 1% DMSO control wells, were also included. Plates were incubated in humid atmosphere, without agitation, at 35 ºC for 48 hours, and the results were read visually, as recommended by the CLSI[71]. MIC was considered the lowest concentration resulting in 100% growth inhibition of yeasts compared to the growth control. MICs of fluconazole and voriconazole against *C. krusei* ATCC 6258, quality control strain, were also performed and the results were within the CLSI proposed limits, considering MIC as 50% growth inhibition. Moreover, FLC (16 to 128 µg/mL) and VOR (0.125 to 16 µg/mL) were used as standard agents, and MIC_{50} and MIC_{100} evaluated.

2.5. Synergistic activity of azoles with amiodarone

The synergistic activity between AMD with two azoles (FLC and VOR) was evaluated against three *Candida* strains following the checkerboard micromethod according to CLSI M27-A3[71], using a sub-inhibitory concentration of AMD. The test was performed in 96-well plates using RPMI 1640 medium (pH 5). It is important to note that the MIC values were also determined for all drugs alone in the same set of experiments in checkerboard assays for comparison. The yeast cell suspensions from SDA cultures were prepared in 0.85% NaCl and the transmittance of cell density adjusted to that produced by a 0.5 McFarland standard. To achieve an inoculum size of $1–5\times10^3$ CFU/mL, the cell suspensions were diluted with RPMI 1640 medium (pH 5). The stock solutions of the drugs were diluted in serial two-folds with RPMI 1640 medium (pH 5) and added to the cell suspensions in order to obtain final concentrations ranging from 0.03–512 µg/mL to FLC, 0.008–64 µg/mL to VOR, and 10 µM to AMD. DMSO was always <1% (v/v) of the total volume of medium. Growth and sterility controls were performed in RPMI 1640 medium (pH 7) with or without 1% DMSO. Plates were incubated at 35 °C for 48 h. Readings of results were performed by visual reading, as recommended by the CLSI[71]. MICs were considered the lowest concentration, alone or in combination, resulting in 100% growth inhibition of yeasts compared to the growth control.

The *in vitro* interactions between the two azoles and AMD were analyzed using a non-parametric model based on Loewe Additivity (LA) theory. The non-parametric approach of LA is based on the fractional inhibitory concentration (FIC) index (FICI) model expressed as the sum of the ratios of the MIC values of each drug when used in combination to their respective MIC values when used alone (**Equation 1**). It was proposed that a FICI <0.5

should be considered “synergism”, a FICI > 4 should be considered “antagonism” and a FICI between 0.5 and 4 should be considered “no interaction”[77].

$$\mathrm{FICI} = \mathrm{FIC_A} + \mathrm{FIC_B} = \frac{\mathrm{MIC_A\ in\ combinatuion}}{\mathrm{MIC_A\ tested\ alone}} + \frac{\mathrm{MIC_B\ in\ combinatuion}}{\mathrm{MIC_B\ tested\ alone}}$$

Equation 1 - Synergism activity evaluated through fractional inhibitory concentration index[77].

2.6. Synergistic activity between azoles and thioxantones

The combined effect of the compounds **Tx 1**, **Tx 2**, **Tx 4**, **Tx 5**, **Tx 7**, **TxA1**, **Tx53**, **TxOMe** and clinically relevant azole antifungal drugs by way of checkerboard micromethod on 96 well plates were performed according to the approved CLSI M27-A3[71]. For the assays, the yeast cell suspensions from SDA cultures were prepared in 0.85% NaCl and the transmittance of cell density adjusted to that produced by a 0.5 McFarland standard. To achieve an inoculum size of 1–5×10^3 CFU/mL, the cell suspensions were diluted with RPMI 1640 medium (pH 7). The stock solutions of all thioxanthones and azoles were diluted in serial two-folds with RPMI 1640 medium (pH 7) and added to the cell suspensions in order to obtain final concentrations ranging from 0.25–128 µg/mL to FLC, 0.03–16 µg/mL to VOR, 16–64 µg/mL to **Tx 1**, **Tx 2**, **Tx 4**, **Tx 5**, **Tx 7**, **Tx53** and **TxOMe**, and 8–64 µg/mL to **Tx53**. DMSO was always <1% (v/v) of the total volume of medium. Growth and sterility controls were performed in RPMI 1640 medium (pH 7) with or without 1% DMSO. Plates were incubated at 35 °C for 48 h. Readings of results were performed by visual reading, as recommended by the CLSI[71]. MICs were considered the lowest concentration, alone or in combination, resulting in 100% growth inhibition of yeasts compared to the growth control.

V. Material and Methods

	1	2	3	4	5	6	7	8	9	10	11	12
A	64	64 + 0.25	64 + 0.5	64 + 1	64 + 2	64 + 4	64 + 8	64 + 16	64 + 32	64 + 64	64 + 128	Growth control
B	32	32 + 0.25	32 + 0.5	32 + 1	32 + 2	32 + 4	32 + 8	32 + 16	32 + 32	32 + 64	32 + 128	Growth control
C	16	16 + 0.25	16 + 0.5	16 + 1	16 + 2	16 + 4	16 + 8	16 + 16	16 + 32	16 + 64	16 + 128	
D		0.25	0.5	1	2	4	8	16	32	64	128	Sterility control
E	64	64 + 0.03	64 + 0.06	64 + 0.125	64 + 0.25	64 + 0.5	64 + 1	64 + 2	64 + 4	64 + 8	64 + 16	Sterility control
F	32	32 + 0.03	32 + 0.06	32 + 0.125	32 + 0.25	32 + 0.5	32 + 1	32 + 2	32 + 4	32 +8	32 + 16	
G	16	16 + 0.03	16 + 0.06	16 + 0.125	16 + 0.25	16 + 0.5	16 + 1	16 + 2	16 + 4	16 + 8	16 + 16	DMSO 1%
H		0.03	0.06	0.125	0.25	0.5	1	2	4	8	16	DMSO 1%

	Tx concentrations (µg/mL)
	FLC concentrations (µg/mL)
	VOR concentrations (µg/mL)

Figure 20 - Checkerboard assay, for combination between **Tx** and azoles.

CHAPTER VI: REFERENCES

VI. References

1. Paiva, A. M.; Pinto, M. M.; Sousa, E., A century of thioxanthones: through synthesis and biological applications. *Current Medicinal Chemistry* **2013,** *20* (19), 2438-57.

2. Graebe, C.; Schultess, O., 1. Ueber Thioxanthon. *Justus Liebigs Annalen der Chemie* **1891,** *263* (1), 1-15.

3. Rosi, D.; Peruzzotti, G.; Dennis, E. W.; Berberian, D. A.; Freele, H.; Archer, S., A new active metabolite of "Miracil D". *Nature* **1965,** *208* (5014), 1005-6.

4. Cioli, D.; Pica-Mattoccia, L.; Archer, S., Antischistosomal drugs: past, present ... and future? *Pharmacology & Therapeutics* **1995,** *68* (1), 35-85.

5. Foster, B. J.; Wiegand, R. A.; Pugh, S.; LoRusso, P. M.; Rake, J.; Corbett, T. H., Pharmacokinetic studies in mice of two new thioxanthenones (183577 and 232759) that showed preferential solid tumor activity. *Clinical cancer research : an official journal of the American Association for Cancer Research* **1997,** *3* (11), 2047-53.

6. Archer, S.; Zayed, A. H.; Rej, R.; Rugino, T. A., Analogues of hycanthone and lucanthone as antitumor agents. *Journal of Medicinal Chemistry* **1983,** *26* (9), 1240-6.

7. Bailly, C.; Waring, M. J., Preferential intercalation at AT sequences in DNA by lucanthone, hycanthone, and indazole analogs. A footprinting study. *Biochemistry* **1993,** *32* (23), 5985-93.

8. Campone, M.; Isambert, N.; Bourbouloux, E.; Maury, S.; Monin-Baroille, P.; Berille, J.; Fumoleau, P., Phase I dose-escalation study of a novel antitumor agent, SR271425, administered intravenously in split doses (d1-d2-d3) in patients with refractory solid tumors. *Cancer Chemotherapy and Pharmacology* **2007,** *59* (5), 689-95.

9. Goncalves, P. H.; High, F.; Juniewicz, P.; Shackleton, G.; Li, J.; Boerner, S.; LoRusso, P. M., Phase I dose-escalation study of the thioxanthone SR271425 administered intravenously once every 3 weeks in patients with advanced malignancies. *Investigational New Drugs* **2008,** *26* (4), 347-54.

10. Lockhart, A. C.; Calvo, E.; Tolcher, A. W.; Rowinsky, E. K.; Shackleton, G.; Morrison, J. G.; Rafi, R.; VerMeulen, W.; Rothenberg, M. L., A phase I dose-escalation study of SR271425, an intravenously dosed thioxanthone analog, administered weekly in patients with refractory solid tumors. *American Journal of Clinical Oncology* **2009,** *32* (1), 9-14.

11. Archer, S.; Pica-Mattoccia, L.; Cioli, D.; Seyed-Mozaffari, A.; Zayed, A. H., The preparation, antischistosomal and antitumor activity of hycanthone and some of its

congeners. Evidence for the mode of action of hycanthone. *Journal of MedicinalCchemistry* **1988,** *31* (1), 254-260.

12. Verbanac, D.; Jain, S. C.; Jain, N.; Chand, M.; Čipčić Paljetak, H.; Matijašić, M.; Perić, M.; Stepanić, V.; Saso, L., An efficient and convenient microwave-assisted chemical synthesis of (thio)xanthones with additional in vitro and in silico characterization. *Bioorganic & Medicinal Chemistry* **2012,** *20* (10), 3180-3185.

13. Bessa, L. J.; Palmeira, A.; Gomes, A. S.; Vasconcelos, V.; Sousa, E.; Pinto, M.; Martins da Costa, P., Synergistic Effects Between Thioxanthones and Oxacillin Against Methicillin-Resistant *Staphylococcus aureus*. *Microbial Drug Resistance (Larchmont, N.Y.)* **2015,** *21* (4), 404-15.

14. Harfenist, M.; Joseph, D. M.; Spence, S. C.; McGee, D. P. C.; Reeves, M. D.; White, H. L., Selective Inhibitors of Monoamine Oxidase. 4. SAR of Tricyclic N-Methylcarboxamides and Congeners Binding at the Tricyclics' Hydrophilic Binding Site. *Journal of Medicinal Chemistry* **1997,** *40* (16), 2466-2473.

15. Lory, P. M. J.; Estrella-Jimenez, M. E.; Shashack, M. J.; Lokesh, G. L.; Natarajan, A.; Gilbertson, S. R., Synthesis and screening of 3-substituted thioxanthen-9-one-10,10-dioxides. *Bioorganic & Medicinal Chemistry Letters* **2007,** *17* (21), 5940-5943.

16. Woo, S.-W.; Kang, D.-H.; Kim, J.-S.; Lee, C.-S.; Lee, E.-S.; Jahng, Y.-D.; Kwon, Y.; Na, Y.-H., *Synthesis, Cytotoxicity and Topoisomerase II Inhibition Study of New Thioxanthone Analogues*. 2008; Vol. 29, p 471-474.

17. Kostakis, I. K.; Pouli, N.; Marakos, P.; Mikros, E.; Skaltsounis, A.-L.; Leonce, S.; Atassi, G.; Renard, P., Synthesis, cytotoxic activity, NMR study and stereochemical effects of some new pyrano[3,2-*b*]thioxanthen-6-ones and Pyrano[2,3-*c*]thioxanthen-7-ones. *Bioorganic & Medicinal Chemistry* **2001,** *9* (11), 2793-2802.

18. Palmeira, A.; Vasconcelos, M. H.; Paiva, A.; Fernandes, M. X.; Pinto, M.; Sousa, E., Dual inhibitors of P-glycoprotein and tumor cell growth: (Re)discovering thioxanthones. *Biochemical Pharmacology l.* **2012,** *83* (1), 57-68.

19. Richardson, M. D., Changing patterns and trends in systemic fungal infections. *The Journal of Antimicrobial Chemotherapy* **2005,** *56 Suppl 1*, i5-i11.

20. Cannon, R. D.; Lamping, E.; Holmes, A. R.; Niimi, K.; Baret, P. V.; Keniya, M. V.; Tanabe, K.; Niimi, M.; Goffeau, A.; Monk, B. C., Efflux-Mediated Antifungal Drug Resistance. *Clinical Microbiology Reviews* **2009,** *22* (2), 291.

21. Prasad, R.; Rawal, M. K., Efflux pump proteins in antifungal resistance. *Frontiers in Pharmacology* **2014,** *5*, 202-202.

22. Pfaller, M. A.; Diekema, D. J., Epidemiology of Invasive Candidiasis: a Persistent Public Health Problem. *Clinical Microbiology Reviews* **2007,** *20* (1), 133.

23. Prasad, R.; Kapoor, K., Multidrug resistance in yeast *Candida*. *International Review of Cytology* **2005,** *242*, 215-48.

24. Loeffler, J.; Stevens, D. A., Antifungal Drug Resistance. *Clinical Infectious Diseases* **2003,** *36*, S31-S41.

25. Zavrel, M.; White, T. C., Medically important fungi respond to azole drugs: an update. *Future Microbiology* **2015,** *10* (8), 1355-73.

26. Sheehan, D. J.; Hitchcock, C. A.; Sibley, C. M., Current and emerging azole antifungal agents. *Clinical Microbiology Reviews* **1999,** *12* (1), 40-79.

27. Mazu, T. K.; Bricker, B. A.; Flores-Rozas, H.; Ablordeppey, S. Y., The Mechanistic Targets of Antifungal Agents: An Overview. *Mini Reviews in Medicinal Chemistry* **2016,** *16* (7), 555-78.

28. Waller, D. G.; Sampson, A. P., 51 - Chemotherapy of infections. In *Medical Pharmacology and Therapeutics (Fifth Edition)*, Waller, D. G.; Sampson, A. P., Eds. Elsevier: 2018; pp 581-629.

29. Victoria Castelli, M.; Gabriel Derita, M.; Noeli Lopez, S., Novel antifungal agents: a patent review (2013 - present). *Expert Opinion on Therapeutic Patents* **2017,** *27* (4), 415-426.

30. Bendel, C. M., CHAPTER 33 - Candidiasis. In *Infectious Diseases of the Fetus and Newborn (Seventh Edition)*, Remington, J. S.; Klein, J. O.; Wilson, C. B.; Nizet, V.; Maldonado, Y. A., Eds. W.B. Saunders: Philadelphia, 2011; pp 1055-1077.

31. Shoham, S.; Groll, A. H.; Petraitis, V.; Walsh, T. J., 156 - Systemic Antifungal Agents. In *Infectious Diseases (Fourth Edition)*, Cohen, J.; Powderly, W. G.; Opal, S. M., Eds. Elsevier: 2017; pp 1333-1344.e4.

32. Taboada, J.; Grooters, A. M., Chapter 9 - Systemic antifungal therapy. In *Small Animal Clinical Pharmacology (Second Edition)*, Maddison, J. E.; Page, S. W.; Church, D. B., Eds. W.B. Saunders: Edinburgh, 2008; pp 186-197.

33. Edwards, J. E., 258 - Candida Species. In *Mandell, Douglas, and Bennett's Principles and Practice of Infectious Diseases (Eighth Edition)*, Bennett, J. E.; Dolin, R.; Blaser, M. J., Eds. Content Repository Only!: Philadelphia, 2015; pp 2879-2894.e3.

34. Kibbler, C. C.; Barton, R.; Gow, N. A. R.; Howell, S.; MacCallum, D. M.; Manuel, R. J., *Oxford Textbook of Medical Mycology*. OUP Oxford: 2017.

35. Vandeputte, P.; Ferrari, S.; Coste, A. T., Antifungal Resistance and New Strategies to Control Fungal Infections. In *International Journal of Microbiology*, 2012.

36. Morio, F.; Jensen, R. H.; Le Pape, P.; Arendrup, M. C., Molecular basis of antifungal drug resistance in yeasts. *International Journal of Antimicrobial Agents* **2017,** *50* (5), 599-606.

37. Calderone, R.; Sun, N.; Weerawarna, P.; Prasad, S.; Gay-Andrieu, F.; Groutas, W.; Alex, D.; Li, D., Antifungal drug discovery: the process and outcomes.

38. Singh, V., Antimicrobial resistance. In *Microbial Pathogens and Strategies for Combating Them: Science, Technology and Education*, Formatex Research Center: 2013; Vol. 1, pp 291–296.

39. WHO. Antimicrobial Resistance. Fact Sheet. Updated February 2018. Available online: https://www.who.int/en/news-room/fact-sheets/detail/antimicrobial-resistance (accessed on 30 March 2019).

40. Transatlantic Taskforce on Antimicrobial Resistance: Progress report May 2014. Available in: https://www.cdc.gov/drugresistance/pdf/TATFAR-Progress_report_2014.pdf (accessed 29 June 2019).

41. *Antibiotic Resistance Threats in the United States, 2013* U.S. Department of Health and Human Services (CDC), 2013.

42. Abdelmohsen, U. R.; Balasubramanian, S.; Oelschlaeger, T. A.; Grkovic, T.; Pham, N. B.; Quinn, R. J.; Hentschel, U., Potential of marine natural products against drug-resistant fungal, viral, and parasitic infections. *The Lancet Infectious Diseases* **2017,** *17* (2), e30-e41.

43. Amaral, L.; Martins, A.; Spengler, G.; Molnar, J., Efflux pumps of Gram-negative bacteria: what they do, how they do it, with what and how to deal with them. *Frontiers in Pharmacology* **2014,** *4*, 168.

44. Holmes, A. R.; Cardno, T. S.; Strouse, J. J.; Ivnitski-Steele, I.; Keniya, M. V.; Lackovic, K.; Monk, B. C.; Sklar, L. A.; Cannon, R. D., Targeting efflux pumps to overcome antifungal drug resistance. *Future Medicinal Chemistry* **2016,** *8* (12), 1485-501.

45. Prasad, R.; Rawal, M. K., Efflux pump proteins in antifungal resistance. *Frontiers in Pharmacology* **2014,** *5*, 202.

46. Wilkens, S., Structure and mechanism of ABC transporters. *F1000prime reports* **2015,** *7*, 14-14.

47. Higgins, C. F., ABC transporters: from microorganisms to man. *Annual Review of Cell Biology* **1992,** *8*, 67-113.

48. Jasinski, M.; Ducos, E.; Martinoia, E.; Boutry, M., The ATP-Binding Cassette Transporters: Structure, Function, and Gene Family Comparison between Rice and Arabidopsis. *Plant Physiology* **2003,** *131* (3), 1169.

49. Davidson, A. L.; Chen, J., ATP-Binding Cassette Transporters in Bacteria. *Annual Review of Biochemistry* **2004,** *73* (1), 241-268.

50. Durães, F.; Pinto, M. M.; Sousa, E., Medicinal Chemistry Updates on Bacterial Efflux Pump Modulators. *Current Medicinal Chemistry* **2018,** *25*, 1-40.

51. Silva, R.; Vilas-Boas, V.; Carmo, H.; Dinis-Oliveira, R. J.; Carvalho, F.; de Lourdes Bastos, M.; Remiao, F., Modulation of P-glycoprotein efflux pump: induction and activation as a therapeutic strategy. *Pharmacology & Therapeutics* **2015,** *149*, 1-123.

52. Vasiliou, V.; Vasiliou, K.; Nebert, D. W., Human ATP-binding cassette (ABC) transporter family. *Human Genomics* **2009,** *3* (3), 281-290.

53. Chen, Z.; Shi, T.; Zhang, L.; Zhu, P.; Deng, M.; Huang, C.; Hu, T.; Jiang, L.; Li, J., Mammalian drug efflux transporters of the ATP binding cassette (ABC) family in multidrug resistance: A review of the past decade. *Cancer Letters* **2016,** *370* (1), 153-164.

54. Decottignies, A.; Goffeau, A., Complete inventory of the yeast ABC proteins. *Nature Genetics* **1997,** *15* (2), 137-45.

55. Coleman, J. J.; Mylonakis, E., Efflux in Fungi: La Pièce de Résistance. *PLoS Pathog.* **2009,** *5* (6), e1000486.

56. Lamping, E.; Baret, P. V.; Holmes, A. R.; Monk, B. C.; Goffeau, A.; Cannon, R. D., Fungal PDR transporters: Phylogeny, topology, motifs and function. *Fungal Genetics and Biology* **2010,** *47* (2), 127-142.

57. Dos Santos, S. C.; Teixeira, M. C.; Dias, P. J.; Sa-Correia, I., MFS transporters required for multidrug/multixenobiotic (MD/MX) resistance in the model yeast: understanding their physiological function through post-genomic approaches. *Frontiers in Physiology* **2014,** *5*, 180.

58. Gulshan, K.; Moye-Rowley, W. S., Multidrug resistance in fungi. *Eukaryot Cell* **2007,** *6* (11), 1933-42.

59. Chen, L.-H.; Tsai, H.-C.; Yu, P.-L.; Chung, K.-R., A Major Facilitator Superfamily Transporter-Mediated Resistance to Oxidative Stress and Fungicides Requires Yap1,

Skn7, and MAP Kinases in the Citrus Fungal Pathogen Alternaria alternata. *PLoS ONE* **2017,** *12* (1), e0169103-e0169103.

60. Monk, B. C.; Niimi, K.; Lin, S.; Knight, A.; Kardos, T. B.; Cannon, R. D.; Parshot, R.; King, A.; Lun, D.; Harding, D. R., Surface-active fungicidal D-peptide inhibitors of the plasma membrane proton pump that block azole resistance. *Antimicrob Agents Chemother* **2005,** *49* (1), 57-70.

61. Goldstein, L. J.; Galski, H.; Fojo, A.; Willingham, M.; Lai, S. L.; Gazdar, A.; Pirker, R.; Green, A.; Crist, W.; Brodeur, G. M.; et al., Expression of a multidrug resistance gene in human cancers. *Journal of the National Cancer Institute* **1989,** *81* (2), 116-24.

62. Palmeira, A.; Sousa, E.; Vasconcelos, M. H.; Pinto, M. M., Three decades of P-gp inhibitors: skimming through several generations and scaffolds. *Current medicinal Chemistry* **2012,** *19* (13), 1946-2025.

63. Varma, M. V.; Ashokraj, Y.; Dey, C. S.; Panchagnula, R., P-glycoprotein inhibitors and their screening: a perspective from bioavailability enhancement. *Pharmacological Research* **2003,** *48* (4), 347-59.

64. Kathawala, R. J.; Gupta, P.; Ashby, C. R., Jr.; Chen, Z. S., The modulation of ABC transporter-mediated multidrug resistance in cancer: a review of the past decade. *Drug resistance updates : reviews and commentaries in antimicrobial and anticancer chemotherapy* **2015,** *18*, 1-17.

65. Aparna, V.; Dineshkumar, K.; Mohanalakshmi, N.; Velmurugan, D.; Hopper, W., Identification of natural compound inhibitors for multidrug efflux pumps of Escherichia coli and Pseudomonas aeruginosa using in silico high-throughput virtual screening and in vitro validation. *PLoS ONE* **2014,** *9* (7), e101840.

66. Marquez, B., Bacterial efflux systems and efflux pumps inhibitors. *Biochimie* **2005,** *87* (12), 1137-47.

67. Alastruey-Izquierdo, A.; Melhem, M. S. C.; Bonfietti, L. X.; Rodriguez-Tudela, J. L., SUSCEPTIBILITY TEST FOR FUNGI: CLINICAL AND LABORATORIAL CORRELATIONS IN MEDICAL MYCOLOGY. *Revista do Instituto de Medicina Tropical de Sao Paulo* **2015,** *57 Suppl 19* (Suppl 19), 57-64.

68. Rex, J. H.; Pfaller, M. A.; Walsh, T. J.; Chaturvedi, V.; Espinel-Ingroff, A.; Ghannoum, M. A.; Gosey, L. L.; Odds, F. C.; Rinaldi, M. G.; Sheehan, D. J.; Warnock, D. W., Antifungal Susceptibility Testing: Practical Aspects and Current Challenges. *Clinical Microbiology Reviews* **2001,** *14* (4), 643.

69. Kontoyiannis, D. P.; Lewis, R. E., Antifungal drug resistance of pathogenic fungi. *The Lancet* **2002,** *359* (9312), 1135-1144.

70. Clinical and Laboratory Standards Institute . Reference Method for Broth Dilution Antifungal Susceptibility Testing of Yeasts; Approved Standard. CLSI document M27-A. Wayne: Clinical and Laboratory Standards Institute; 1997.

71. Clinical and Laboratory Standards Institute . Reference Method for Broth Dilution Antifungal Susceptibility Testing of Yeast; Approved Standard-Third Edition. CLSI document M27-A3. Wayne: Clinical and Laboratory Standards Institute; 2008.

72. Clinical and Laboratory Standards Institute . Reference Method for Broth Dilution Antifungal Susceptibility Testing of Filamentous Fungi; Approved Standard-Second Edition. CLSI document M38-A2. Wayne: Clinical and Laboratory Standards Institute; 2008.

73. Paiva, A. M.; Pinto, M. M.; Sousa, E., A Century of Thioxanthones: Through Synthesis and Biological Applications. *Current Medicinal Chemistry* **2013,** *20* (19), 2438-2457.

74. Nandwana, N. K.; Dhiman, S.; Shelke, G. M.; Kumar, A., Copper-catalyzed tandem Ullmann type C-N coupling and dehydrative cyclization: synthesis of imidazo[1,2-c]quinazolines. *Organic & Biomolecular Chemistry* **2016,** *14* (5), 1736-41.

75. Sambiagio, C.; Marsden, S. P.; Blacker, A. J.; McGowan, P. C., Copper catalysed Ullmann type chemistry: from mechanistic aspects to modern development. *Chemical Society Reviews* **2014,** *43* (10), 3525-3550.

76. Grossman, O.; Azerraf, C.; Gelman, D., Palladium Complexes Bearing Novel Strongly Bent Trans-Spanning Diphosphine Ligands: Synthesis, Characterization, and Catalytic Activity. *Organometallics* **2006,** *25* (2), 375-381.

77. Mukherjee, P. K.; Sheehan, D. J.; Hitchcock, C. A.; Ghannoum, M. A., Combination treatment of invasive fungal infections. *Clinical Microbiology Reviews* **2005,** *18* (1), 163-194.

78. da Silva, C. R.; de Andrade Neto, J. B.; Sidrim, J. J.; Angelo, M. R.; Magalhaes, H. I.; Cavalcanti, B. C.; Brilhante, R. S.; Macedo, D. S.; de Moraes, M. O.; Lobo, M. D.; Grangeiro, T. B.; Nobre Junior, H. V., Synergistic effects of amiodarone and fluconazole on *Candida tropicalis* resistant to fluconazole. *Antimicrobial Agents and Chemotherapy* **2013,** *57* (4), 1691-700.

79. Gamarra, S.; Rocha, E. M. F.; Zhang, Y.-Q.; Park, S.; Rao, R.; Perlin, D. S., Mechanism of the synergistic effect of amiodarone and fluconazole in *Candida albicans. Antimicrobial Agents and Chemotherapy* **2010,** *54* (5), 1753-1761.

80. Courchesne, W. E., Characterization of a novel, broad-based fungicidal activity for the antiarrhythmic drug amiodarone. *The Journal of Pharmacology and Experimental Therapeutics* **2002,** *300* (1), 195-9.

81. Zhang, Y. Q.; Rao, R., Global disruption of cell cycle progression and nutrient response by the antifungal agent amiodarone. *The Journal of Biological Chemistry* **2007,** *282* (52), 37844-53.

82. Afeltra, J.; Vitale, R. G.; Mouton, J. W.; Verweij, P. E., Potent synergistic in vitro interaction between nonantimicrobial membrane-active compounds and itraconazole against clinical isolates of *Aspergillus fumigatus* resistant to itraconazole. *Antimicrobial Agents and Chemotherapy* **2004,** *48* (4), 1335-43.

83. Gupta, S. S.; Ton, V. K.; Beaudry, V.; Rulli, S.; Cunningham, K.; Rao, R., Antifungal activity of amiodarone is mediated by disruption of calcium homeostasis. *The Journal of Biological Chemistry* **2003,** *278* (31), 28831-9.

84. Guo, Q.; Sun, S.; Yu, J.; Li, Y.; Cao, L., Synergistic activity of azoles with amiodarone against clinically resistant *Candida albicans* tested by chequerboard and time-kill methods. *Journal of Medical Microbiology* **2008,** *57* (Pt 4), 457-62.

85. Muend, S.; Rao, R., Fungicidal activity of amiodarone is tightly coupled to calcium influx. *FEMS Yeast Res* **2008,** *8* (3), 425-31.

86. Fisher, M. C.; Henk, D. A.; Briggs, C. J.; Brownstein, J. S.; Madoff, L. C.; McCraw, S. L.; Gurr, S. J., Emerging fungal threats to animal, plant and ecosystem health. *Nature* **2012,** *484*, 186.

87. Pfaller, M. A.; Diekema, D. J., Epidemiology of invasive candidiasis: a persistent public health problem. *Clinical Microbiology Reviews* **2007,** *20* (1), 133-63.

88. Whaley, S. G.; Berkow, E. L.; Rybak, J. M.; Nishimoto, A. T.; Barker, K. S.; Rogers, P., Azole antifungal resistance in *Candida albicans* and emerging non-*albicans Candida* Species. *Frontiers in Microbiology* **2017,** *7* (2173).

89. Knorre, D. A.; Krivonosova, T. N.; Markova, O. V.; Severin, F. F., Amiodarone inhibits multiple drug resistance in yeast *Saccharomyces cerevisiae*. *Archives of Microbiology* **2009,** *191* (8), 675-9.

90. Mai, A.; Rotili, D.; Massa, S.; Brosch, G.; Simonetti, G.; Passariello, C.; Palamara, A. T., Discovery of uracil-based histone deacetylase inhibitors able to reduce acquired antifungal resistance and trailing growth in Candida albicans. *Bioorganic & Medicinal Chemistry Letters* **2007,** *17* (5), 1221-5.

91. Du, D.; Wang-Kan, X.; Neuberger, A.; van Veen, H. W.; Pos, K. M.; Piddock, L. J. V.; Luisi, B. F., Multidrug efflux pumps: structure, function and regulation. *Nature Reviews Microbiology* **2018,** *16* (9), 523-539.

92. Rocha, M. F. G.; Bandeira, S. P.; de Alencar, L. P.; Melo, L. M.; Sales, J. A.; Paiva, M. d. A. N.; Teixeira, C. E. C.; Castelo-Branco, D. d. S. C. M.; Pereira-Neto, W. d. A.; Cordeiro, R. d. A.; Sidrim, J. J. C.; Brilhante, R. S. N., Azole resistance in C*andida albicans* from animals: Highlights on efflux pump activity and gene overexpression. *Mycoses* **2017,** *60* (7), 462-468.

93. Holmes, A. R.; Keniya, M. V.; Ivnitski-Steele, I.; Monk, B. C.; Lamping, E.; Sklar, L. A.; Cannon, R. D., The Monoamine Oxidase A Inhibitor Clorgyline Is a Broad-Spectrum Inhibitor of Fungal ABC and MFS Transporter Efflux Pump Activities Which Reverses the Azole Resistance of Clinical Isolates. *Antimicrobial Agents and Chemotherapy* **2012,** *56* (3), 1508.

94. Lopes, A.; Martins, E.; Silva, R.; Pinto, M. M. M.; Remiao, F.; Sousa, E.; Fernandes, C., Chiral Thioxanthones as Modulators of P-glycoprotein: Synthesis and Enantioselectivity Studies. *Molecules* **2018,** *23* (3).